EarthArXiv Coversheet

April 27th, 2026

Title:

Evaluating Sampling Bias and Model Uncertainty in Species Distribution Models of Marine Plankton Using Virtual Ecosystem Data

Authors:

Zhibo Shao[1], B. B. Cael[2,4], Thelma Panaïotis[2], Anna E. Hickman[1], Stephanie Dutkiewicz[3], Ben A. Ward[1]

Affiliations:

1. Ocean and Earth Science, University of Southampton, SO14 3ZH Southampton, United Kingdom.
2. Ocean Biogeochemistry and Ecosystems, National Oceanography Centre, Southampton, SO14 3ZH, United Kingdom.
3. Department of Earth, Atmospheric and Planetary Sciences, Massachusetts Institute of Technology, Cambridge, MA, USA.
4. Department of the Geophysical Sciences, University of Chicago, IL, USA.

Corresponding author:

Zhibo Shao (Z.Shao@soton.ac.uk)

Running head:

Bias and Uncertainty in Species Distribution Models

Keywords:

Species distribution model, Plankton biogeography, Model evaluation, Bias-variance trade-off, Biogeochemical modelling

Evaluating Sampling Bias and Model Uncertainty in Species Distribution Models of Marine Plankton Using Virtual Ecosystem Data

Zhibo Shao [1], B. B. Cael [2,4], Thelma Panaïotis [2], Anna E. Hickman [1], Stephanie Dutkiewicz [3], Ben A. Ward[1]

[1] Ocean and Earth Science, University of Southampton, SO14 3ZH Southampton, United Kingdom

[2] Ocean Biogeochemistry and Ecosystems, National Oceanography Centre, Southampton, SO14 3ZH, United Kingdom

[3] Department of Earth Atmosphere and Planetary Sciences, Massachusetts Institute of Technology, Cambridge, Massachusetts, USA

[4] Department of the Geophysical Sciences, University of Chicago, IL, USA

Corresponding authors:

Zhibo Shao (Z.Shao@soton.ac.uk)

Running head: Bias and Uncertainty in Species Distribution Model

Keywords: Species distribution model, Plankton biogeography, Model evaluation, Bias-Variance Trade-off, Biogeochemical modelling

Abstract

Understanding the biodiversity and biogeography of plankton in the ocean is essential for predicting responses to environmental changes and informing ocean conservation and management strategies. Species distribution models (SDMs) are a pivotal tool in this regard. This study used data from a global marine ecosystem model as a testbed to assess the reliability of various SDMs, including Generalized Linear Model (GLM), Generalized Additive Model (GAM), Random Forest (RF), Boosted Regression Trees (BRT) and Artificial Neural Network (ANN). We used artificial datasets to replicate the sampling patterns of three datasets: a compiled dataset of global scope, the Tara Ocean dataset, and the Atlantic Meridional Transect (AMT) project. Our findings indicate that tree-based algorithms, RF and BRT, exhibit better predictive accuracy and stability compared to GLM, GAM, and ANN, especially when trained with more spatially resolved datasets. We highlight the significant influence of sampling bias on model performance, with models trained on more comprehensive global datasets outperforming those trained on more latitudinally and longitudinally biased data respectively (Tara and AMT). Furthermore, we demonstrate that broad spatial coverage is a more critical determinant of predictive skill than sample size alone, as simply increasing sampling density within a biased region is insufficient to overcome poor spatial representation. Overall, this research underscores the necessity of careful consideration of sampling strategies and model selection in plankton species distribution modelling.

1. Introduction

The diversity of marine plankton is important in sustaining and mediating important ecosystem functions. A broader spectrum of diversity can bolster the functional resistance of communities to varying environments (Baert et al., 2016) and control marine biogeochemistry (Le Quéré et al., 2016; Litchman et al., 2015). Since phytoplankton groups differ in their size, nutrient stoichiometry and acquisition traits, shifts in community composition and species distributions can profoundly influence global biogeochemical cycles and marine foodwebs. Therefore, describing the patterns of plankton biodiversity and biogeography is crucial for understanding how plankton communities shape ecological dynamics across oceanic regions (Frémont et al., 2023; Villarino et al., 2015).

Species distribution models (SDMs) are used in ecology and conservation biology to predict and analyse species' geographic distributions and suitable habitats (Melo-Merino et al., 2020; Robinson et al., 2017). SDMs rely on ecological niche theory (Elith and Franklin, 2017), and in particular exploit Hutchinson's definition of the niche as an "n-dimensional hypervolume" that describes the range of environmental conditions (e.g. temperature, food availability, competition, predation) in which a particular species (or other group of organisms) is found (Hutchinson, 1957). SDMs encompass a wide variety of algorithms, ranging from simpler methods like generalized linear model (GLM) to more complex machine learning approaches such as random forest (RF) and boosted regression tree (BRT). These algorithms differ in their assumptions, complexity, and ability to capture non-linear relationships, which can influence their predictive performance in different ecological contexts.

SDMs have become a vital tool for mapping plankton biogeography, with studies varying widely in scope and objective. A significant body of research has focused on predicting global distributions. For instance, studies have used niche modeling to map the worldwide

habitats of cyanobacteria like *Prochlorococcus* and *Synechococcus* (Flombaum et al., 2013; Flombaum et al., 2020), coccolithophores (O'brien et al., 2013), and diazotrophs (Tang and Cassar, 2019). Others have used ensemble approaches, which combine multiple SDMs, to create robust global predictions for diverse plankton assemblages (Benedetti et al., 2021). Another critical application is projecting distributions into the future ocean to forecast the impacts of climate change. Studies have used SDMs to predict how the distributions of North Atlantic phytoplankton (Barton et al., 2016) and zooplankton communities (Villarino et al., 2015) might shift. Similarly, researchers have forecasted the restructuring of plankton genomic biogeography (Frémont et al., 2022) and assessed the tipping points of phytoplankton in response to multiple environmental stressors (Ban et al., 2022). Many studies also use SDMs to identify the key environmental drivers shaping these distributions. For instance, BRT is used to identify drivers for Southern Ocean zooplankton (Pinkerton et al., 2010), while RF has identified drivers for picophytoplankton in the South China Sea (Chen et al., 2020).

A common thread in this body of work is that studies typically select a single preferred SDM or use an ensemble of multiple models to generate a consensus prediction (Bourel et al., 2017). However, the use of SDMs is subject to many assumptions and uncertainties, as reviewed by (Wiens et al., 2009), and a systematic investigation into the fundamental assumptions and uncertainties inherent in these different algorithmic choices is often missing - a challenge noted in earlier work that found the predictive skill of SDMs for plankton can be limited (Brun et al., 2016).

Sampling bias can greatly influence the predictive skills of SDMs (Bardon et al., 2021; Guillera-Arroita et al., 2015; Hughes et al., 2021). When sampling bias exists in the SDMs, estimated relationships would largely depend on the environment in the sampled area, making the models less applicable across broader scales (Hughes et al., 2021). Moreover, environments

that are not sampled may remain unrepresented in the estimated niche space, which can lead to inaccurate predictions when models are applied to novel environments or extrapolated beyond the range of sampled conditions. This highlights the inherent limitations of extrapolation in SDMs (Hernandez et al., 2006).

Given the wide choice of SDM algorithms available, it is also meaningful for us to test whether SDMs vary in their ability to represent planktonic biogeography, both in the present day and in response to future change. For instance, GLMs assume linear relationships between predictors and the response variable, offering straightforward interpretation but limited flexibility for complex ecological patterns. In contrast, GAMs extend GLMs by allowing for non-linear relationships through smooth functions, making them better suited for data exhibiting non-linear relationships. Tree-based ensembles include RF, which build multiple independent trees on random subsets of the data and average their predictions to reduce variance and prevent overfitting. BRT also use an ensemble of trees but build them sequentially, with each new tree iteratively refining predictions by focusing on harder-to-predict cases. Finally, Artificial Neural Networks (ANN), a multilayer perceptron, can capture highly complex, high-dimensional relationships, but their intricate structure can make it more challenging to interpret than the other models.

The established approach of evaluating SDMs is constrained by significant uncertainties, including the risk of overfitting specific datasets and limited applicability across broader spatiotemporal scales. To address these limitations, we apply an alternative approach, using output from a global ecosystem model output as a ‘virtual world’ testbed for evaluating SDM performance. Subsampling model output in place of real-world observations allows for an internally consistent comparison of SDM performance. This approach enables us to test SDM performance using various realistic sampling strategies against a perfect 'ground truth' (the full model output) that offers global coverage, lacks experimental errors, and is available

for both present and future climate scenarios. Using this approach, Bardon et al. (2021) demonstrated that GAMs, a commonly used type of SDM, face considerable challenges in accurately predicting the future biomass distribution of phytoplankton when evaluated using a future climate change simulation.

Here we extend the work of Bardon et al. (2021) to compare the skill of five SDMs across a range of complexities, identifying factors influencing their performance, and exploring methods that might enhance their accuracy. Our study builds on their findings by broadening the range of SDM types evaluated and systematically exploring the impact of species distribution model complexity, bias, and variance on predictive skill. Additionally, we address the challenges of spatiotemporal extrapolation by incorporating more complex sampling scenarios and analyzing how spatial and temporal resolution of training data affects SDM performance across various functional groups of plankton. In the following, Section 2 provides a detailed description of the artificial ecosystem that we use as a testbed, describes how this model is sampled to replicate real-world observation strategies, and introduces the SDMs under assessment. Section 3 presents a performance comparison across the SDMs and explores the sensitivity to spatiotemporal biases in the training data. Section 4 discusses a trade-off between bias and variance in SDMs of differing complexity and examines the key factors influencing SDM performance.

2 Materials and Procedures

2.1 Data access

Following Bardon et al. (2021), we generated artificial ecosystem data from a 3 dimensional global physical-biogeochemical-ecosystem model (Darwin) simulation designed to explore diversity and community structure changes in a future world (Cael et al., 2021; Henson et al., 2021). This ecosystem model simulates marine microbes and biogeochemical cycles, within a

physical ocean environment provided by the Massachusetts Institute of Technology General Circulation Model (MITgcm) (Marshall et al., 1997), coupled to a earth system of intermediate complexity (Monier et al., 2018) to provide a future change scenario under high emissions (similar to IPCC's Representative Concentration Pathway 8.5 (RCP8.5) (Riahi et al., 2011).

The ecosystem model itself represents a complex ecosystem with a detailed plankton community structure (Dutkiewicz et al., 2021). It explicitly simulates dozens of distinct phytoplankton types and multiple zooplankton grazers, which are further categorized into broader plankton functional types (PFTs) based on traits like size and biogeochemical function. The version used for this study includes 51 plankton, ranging in size from 0.6 to 2.4 mm and classified into seven PFTs: **prok**aryotes, **pico**eukaryotes, **cocco**lithophores, **diat**oms, **dino**flagellates, **diazo**trophs, and **zoop**lankton (abbreviations in bold). The simulation was first driven by physical forcing consistent with observed greenhouse gas emission concentrations from 1860 to 1990 and and subsequently with high emissions from 1990 to 2110 (Riahi et al., 2011). This setup captures natural variability (e.g. El Nino) consistent with the real world and projects future changes in ocean conditions. We focus here only on the model output from the latter component of the simulation (1990-2100) for consistency in the forcing. This virtual world allowing us to evaluate SDM performance across a wide range of environmental scenarios, including those induced by climate change. The ocean environment is represented across a 2° latitude by 2.5° longitude grid, and simulates environmental variables, which serve as predictors in SDMs, including monthly surface (0-10 m) values of temperature (SST), salinity (SSS), nitrate (NO_3), phosphate (PO_4), dissolved iron (dFe), silicate (Sil), and photosynthetically active radiation (PAR).

To closely replicate real-world ocean sampling and examine the spatial-temporal effects on SDM performance, we retrieved environmental data and population biomasses from the model

at the times and locations corresponding to those of three different observational datasets (Fig. 1):

1. **Global:** A comprehensive database based on a compilation of global picoplankton observations (Flombaum et al., 2020). This dataset includes samples from 39 research cruises covering all major oceanographic environments. It is therefore representative of the current level of *in situ* coverage of the global ocean for the picoplankton sub-group**.**
2. **Tara:** Observations from the Tara Ocean project (Sunagawa et al., 2015); The Tara Ocean project is a global initiative designed to explore plankton diversity and ocean ecosystems. Sampling was conducted across multiple ocean basins, with a focus on a wide range of environmental gradients. While polar environments are represented, there is a bias in sampling density towards lower latitudes.
3. **AMT:** 30 transects from the Atlantic Meridional Transect (AMT) project (Rees et al., 2024). The AMT project focuses on repeated sampling along a latitudinal transect in the Atlantic Ocean, covering a diverse range of environments from temperate to tropical and equatorial regions. These transects provide high-resolution, longitudinal data over a wide range of oceanographic conditions within the Atlantic Ocean.

Observations were taken from the model surface layer, with data in coastal areas (depth < 200m) excluded. Coastal areas were excluded to focus on open-ocean dynamics and avoid the confounding influence of localized processes, such as riverine inputs, upwelling, and tidal mixing (Gattuso et al., 1998; Simpson and Sharples, 2012), which the model with its coarse

resolutions does not capture. Details, including the number of observations in each dataset, are given in Table 1.

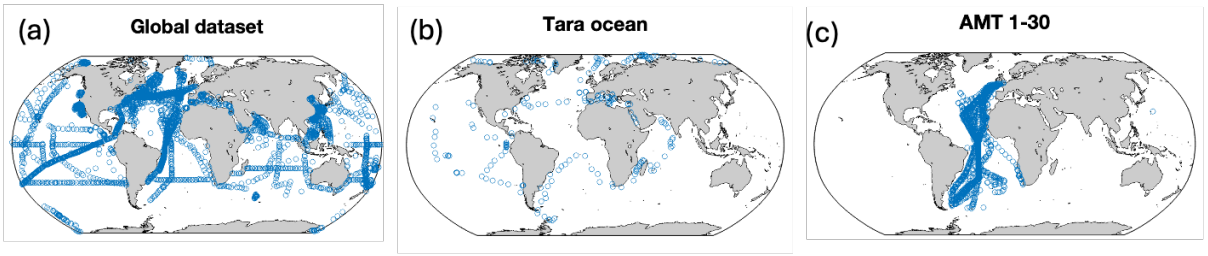

Figure 1: The sampling points of the Global dataset (a), the Tara Ocean dataset (b) and AMT projects dataset (c).

The model data were extracted and split into two sets: the present dataset (1991-2011, the first 21 years of the ecosystem model run with emission scenario) and the future dataset (2079-2099). A temporal adjustment was necessary to apply the sampling scheme of the compiled global dataset (originally collected 1987–2008) to our model's 'present-day' simulation period (1991–2011). To achieve this, for each data point in the observational dataset, we retained its original spatial coordinates and calendar month. However, we shifted its year forward by four years to align with our model's timeline. For instance, a sample originally collected at a specific location in May 1987 was replicated by extracting data from our model at the same location in May 1991. This method preserves the spatial and seasonal structure of the real-world sampling effort while ensuring its compatibility with the temporal bounds of our virtual ecosystem.

2.2 Species distribution model choice

We selected five species distribution models used in previous studies including a generalized linear model (GLM) (Mccullagh, 1989) and a generalized additive model (GAM) (Hastie, 1990); two decision-tree-based algorithms - a random forest (RF) (Breiman, 2001) and a

boosted regression tree (BRT) (Elith et al., 2008); and one deep learning algorithm - an artificial neural network (ANN) (Hornik et al., 1989).

The varying complexity of the selected SDMs necessitated two distinct training procedures. The parametric models (GLM and GAM) do not require hyperparameter optimization and were therefore trained directly on the full training dataset. For the GAM, the number of permitted splines was set to 20 for each predictor variable, following Bardon et al. (2021), who demonstrated that model sensitivity to this parameter is negligible.

Conversely, more complex machine learning models (RF, BRT, and ANN) required hyperparameter tuning to prevent overfitting. We employed a grid search with 8-fold cross-validation to identify the optimal configurations (Fig. S1; see the Supplementary Material for justification of fold selection, Fig. S2). We evaluated 81 (3^4) hyperparameter combinations for RF and BRT, and 27 (3^3) for the ANN (Table S1). The configuration yielding the RMSE across the validation folds was selected. Crucially, once these optimal hyperparameters were determined, the final RF, BRT, and ANN models were retrained on the entire, unsplit training dataset using these specific configurations.

This ensures that, despite the differing development processes, the final models for all five algorithms were trained on the exact same dataset. Consequently, the final evaluation was unbiased: all five fully trained models were assessed on the same, completely global test set.

Additionally, we conducted 100-times bootstrap analyses to evaluate the resilience of the SDMs to noise or fluctuations in varying datasets, which helps in assessing their robustness against variation error. In every bootstrap sampling, we randomly selected n data points from the original dataset (with replacement), where n is the total number of samples in the original dataset**.**

2.3 Scenario design

To examine the temporal and spatial effects of the real-world sampling efforts on SDM prediction performance, we sampled the global ecosystem model several different ways (Table 1). In the first set of scenarios, we sampled the virtual ecosystem model at the times and locations of observations in the Global dataset (Global dataset, Fig. 1a), Tara Oceans (Tara, Fig. 1b) and Atlantic Meridional Transect (AMT, Fig. 1c) projects (based on monthly average and 2°×2.5° degree ecosystem model resolution).

To specifically investigate the influence of temporal sampling resolution on model performance, we designed two additional training datasets using the Tara Ocean sampling scheme as a baseline. The Tara dataset was chosen for these sensitivity tests because it lacks both inter-annual and intra-annual replication, making it a suitable baseline for evaluating how increasing temporal resolution in either dimension influences model performance. The two new training scenarios were constructed as follows: **Tara-12months (Intra-annual variability) -** to simulate comprehensive seasonal coverage, we took each spatial location from the original Tara dataset and sampled our virtual model once for every calendar month within a single, representative year. This generated a new training dataset with dense seasonal information at the original Tara locations. **Tara-12yrs (Inter-annual variability)** - to simulate a long-term monitoring effort, we took each original Tara sample (location and month) and repeated the sampling in the same month and location across twelve consecutive years. This created a training dataset rich in year-to-year information but with the same sparse seasonal coverage as the original. These two datasets were then used to train the SDMs, allowing us to directly evaluate whether resolving seasonal dynamics or capturing long-term inter-annual trends is more beneficial for improving model performance."

In a further set of scenarios, we assessed the impact of spatial variability to determine how model performance changes when sampling effort remains constant but spatial bias is removed. Following a similar approach to Bardon et al. (2021), whereby locations and

sampling months were randomly sampled within the same time period of original global (Global-random) and Tara datasets (Tara-random) (Fig. S3a and b). In each random dataset, each data point's location and sampling time were randomly selected. The locations were selected at random with uniform probability across the global ocean surface, while the sampling times were randomly chosen within the time span corresponding to the original global and Tara datasets. Additionally, the number of samples matches that of the original dataset.

To explicitly disentangle the effects of sample size from spatial sampling bias, we created two new training datasets based on a "densified sampling" approach (Fig. S3c and d). These new datasets, hereafter referred to as Tara-densified and AMT-densified, were designed to increase the sample sizes of the Tara and AMT scenarios to be comparable with the Global dataset while preserving their original spatial biases. The densification was achieved by expanding the sampling at each original station location. For every data point in the original Tara and AMT datasets, we sampled not only that grid cell but also adjacent grid cells in the model output. This process resulted in an increase in the number of samples for each dataset, bringing their total sample sizes into a range comparable to that of the Global dataset. This experimental design allows for a direct test of whether increasing sampling density along a biased transect can overcome the limitations imposed by poor spatial coverage.

Finally, for the test dataset, we evaluated SDM performance by validating the SDMs' present and future predictions against the known 'ground truth' biomass from the ecosystem model simulation.

Table 1 Summary of datasets used in SDMs

Dataset	Data description	Purpose	No. of grid cells	Time span
Training data				

Global dataset	Data were sampled in the same location and time as the records in meta-database	Examine the SDM accuracy (Section 3.1 & 3.2)	3,167	1991 – 2012
Tara	Data were sampled in the same location and time as the records in Tara Ocean projects		131	2009 – 2013
AMT	Data were sampled in the same location and time as the records in all AMT 1-30 transects		1,224	1995 – 2023
Tara-12yrs	Data were sampled in the same location and months as the records in Tara Ocean projects across twelve consecutive years	Examine the influence of temporal variation (Section 3.2)	1,512	2002 – 2013
Tara-12mths	Data were sampled repeatedly in every month of the sampling year with the same location as the records in Tara Ocean projects		1,512	2009 – 2013
Global-random	Data were sampled randomly and uniformly with the same sample size of the global dataset	Examine the influence of spatial variation (Section 4.3)	3,167	1991 – 2012
Tara-random	Data were sampled randomly and uniformly with the same sample size of the Tara Ocean dataset		131	2009 – 2013
Tara-densified	Data were sampled at each original Tara location and its eight adjacent grid cells to increase sample density.	Examine if increased sample size can overcome spatial bias.	3,304	2009 – 2013
AMT-densified	Data were sampled at each original AMT location and its eight adjacent grid cells to increase sample density.	Examine if increased sample size can overcome spatial bias.	2,935	1995 – 2023
Test data				
Present	The whole ocean data in first 21 years of virtual ecosystem models (1991 ~ 2011)	Examine the SDM performance	1,793,527	1991 – 2011

Future	The whole ocean data in last 21 years of virtual ecosystem models (2079 ~ 2099)	of present and future predictions	1,793,527	2079 – 2099

294

295 **3 Assessment**

296 **3.1 Performance of the five SDMs**

297 We first present results from training the five different SDMs on the three datasets, assessing
298 performance against training and test data. Although the SDMs were trained to seven PFTs, we
299 presented results for picoeukaryotes in this section for simplicity. Results for the remaining
300 species are provided in the supplementary materials (Fig. S4-S10), and the main conclusions
301 remain consistent across all PFTs, without affecting the key findings in Sect. 3.1 and Sect. 3.2.

302 In the following we use Taylor diagrams (Taylor, 2001) to summarise three (inter-related)
303 aspects of model performance with regard to the training and test data. For each model
304 evaluation, the normalised standard deviation of the model (relative to the standard deviation
305 of the artificial data) is indicated as the radial distance from the pole (or origin). Simultaneously,
306 the correlation between the model and the artificial observations is indicated by the angular
307 distance from the vertical axis. The RMSD (Root Mean Square Differences) between the model
308 and artificial data is given as a third (non-independent) metric, as indicated by the radial
309 distance from a point where the RMSD is zero. This point corresponds to a perfect model (for
310 which every predicted value is identical to the observations), and is therefore located where the
311 normalised standard deviation and correlation coefficient are both equal to one (as indicated
312 by the red dot in each panel of Figure 2). The locations of the points, each representing a single
313 SDM bootstrap iteration, thus indicate the strength of the correlation, the overall distance from
314 the observations, and whether the variability in the model is larger (normalised s.d > 1) or
315 smaller (normalised s.d < 1) than in the artificial observations. A normalized standard deviation

316 greater than 1 indicates the model overestimates variability, while a value less than 1 indicates
317 underestimation, which may smooth out fine-scale patterns.

318 When trained to the Global dataset, the RF and BRT performed the best with regard to the
319 training data, with very high correlations and only slightly underestimating the variance in the
320 artificial data (open yellow and orange points in Fig. 2a). The ANN also performed well (open
321 blue points in Fig. 2a), with only a slightly lower correlation and similar variance (although
322 isolated bootstraps performed extremely poorly (single point with a correlation of 0.3 in
323 Fig. 2a). The simpler GAM and GLM models showed lower correlations and underestimated
324 the variance of the training data (open green and purple points in Fig. 2a). The GLM was
325 particularly poor in this regard, showing a low correlation and unrealistically low variance.

326 When the five globally trained SDMs were evaluated against the test data (closed circles in Fig.
327 2a), the models ranked in the same order as against the training data, in terms of correlation
328 and RMSD. While the performance of best four models all deteriorated in terms of correlation
329 and RMSD with the shift from training to test data, the performance of the GLM improved
330 slightly (although it was still worst among the five models).

331 When the SDMs were trained to the more spatially restricted AMT (Fig. 2b) and Tara datasets
332 (Fig. 2c), the ANN was best able to reproduce the training data, closely followed by the BRT,
333 RF and GAM. All four of these models had very high correlations and closely reproduced the
334 degree of variance in the artificial data. In contrast the GLM again had a much lower correlation
335 and underestimated the variance of the training data.

336 In contrast to the global datasets, the performance of the ANN and GAM, trained by Tara and
337 AMT datasets (open blue and purple circles in Fig. 2b,c), deteriorated massively when
338 evaluated against the test data (solid blue and purple circles in Fig. 2b,c). All 100 bootstraps
339 had lower correlations and higher RMSD compared to the performance against the training

data, and almost all showed artificially high variance. These results indicate that the ANN and GAM were significantly overfitting the training data, leading to poorly constrained and highly variable model predictions.

The GLM (green points in Fig. 2) also performed poorly with regard to the three sets of training data, but this was associated with a consistently low correlation, with much less variability in performance. When the AMT-trained model was evaluated against the test data the correlation was extremely low, but with much lower variance than exhibited by the predictions of the ANN (blue points) and GAM (purple points). This perhaps suggests that the GLM was underfit, leading to high bias error with low variance. The GLM had a slightly lower predictive bias when trained to the Tara data, but the variability in its predictions was higher.

Among the evaluated SDMs, the GLM consistently performed the worst (green points), both against the training data and test data. Although ANN (blue points) and GAM (purple points) captured variance well within the training data, their performance was less stable in terms of the test data, especially in the AMT and Tara cases, where the outcomes were subject to very high uncertainty in response to random changes in the sampling of the training data. In contrast, across all three cases, the decision-tree-based methods (RF and BRT) demonstrated more consistent and stable performance, showing lower variance and better overall reliability, especially in terms of their performance against the test data.

Overall, RF and BRT are well-suited for our specific cases due to their accurate performance and lower variance. Although the SDMs were trained on all seven plankton functional groups, we present the results for picoeukaryotes in this section for simplicity, with the results for the remaining PFTs provided in the supplementary materials (Fig. S4–S10). While the exact positions of the points on the Taylor diagrams may differ for other PFTs, the key patterns and conclusions remain consistent. Specifically, across all functional groups, the GAM and ANN

models consistently exhibit a highly scattered pattern for the test data, indicating high variance and instability. Furthermore, the relative performance ranking of the models is preserved across all PFTs, with RF and BRT consistently showing the most robust performance. Therefore, our main findings in this section are not altered by the choice of PFT shown.

To provide a more quantitative summary of these results, the RMSD for both training and test datasets are plotted against each other for all seven PFTs (Figure S11). This figure directly visualizes the degree of model overfitting, where points lying above the 1:1 line indicate that the test error is higher than the training error. As expected, all models show some degree of overfitting, but this is particularly pronounced for the ANN and GAM models, which consistently fall far above the 1:1 line, especially when trained on the spatially biased Tara and AMT datasets. In contrast, the RF and BRT models, particularly when trained on the Global dataset, lie closer to the 1:1 line and closer to the origin, quantitatively confirming their lower overall error and greater robustness against overfitting. This pattern is consistent across all plankton functional groups.

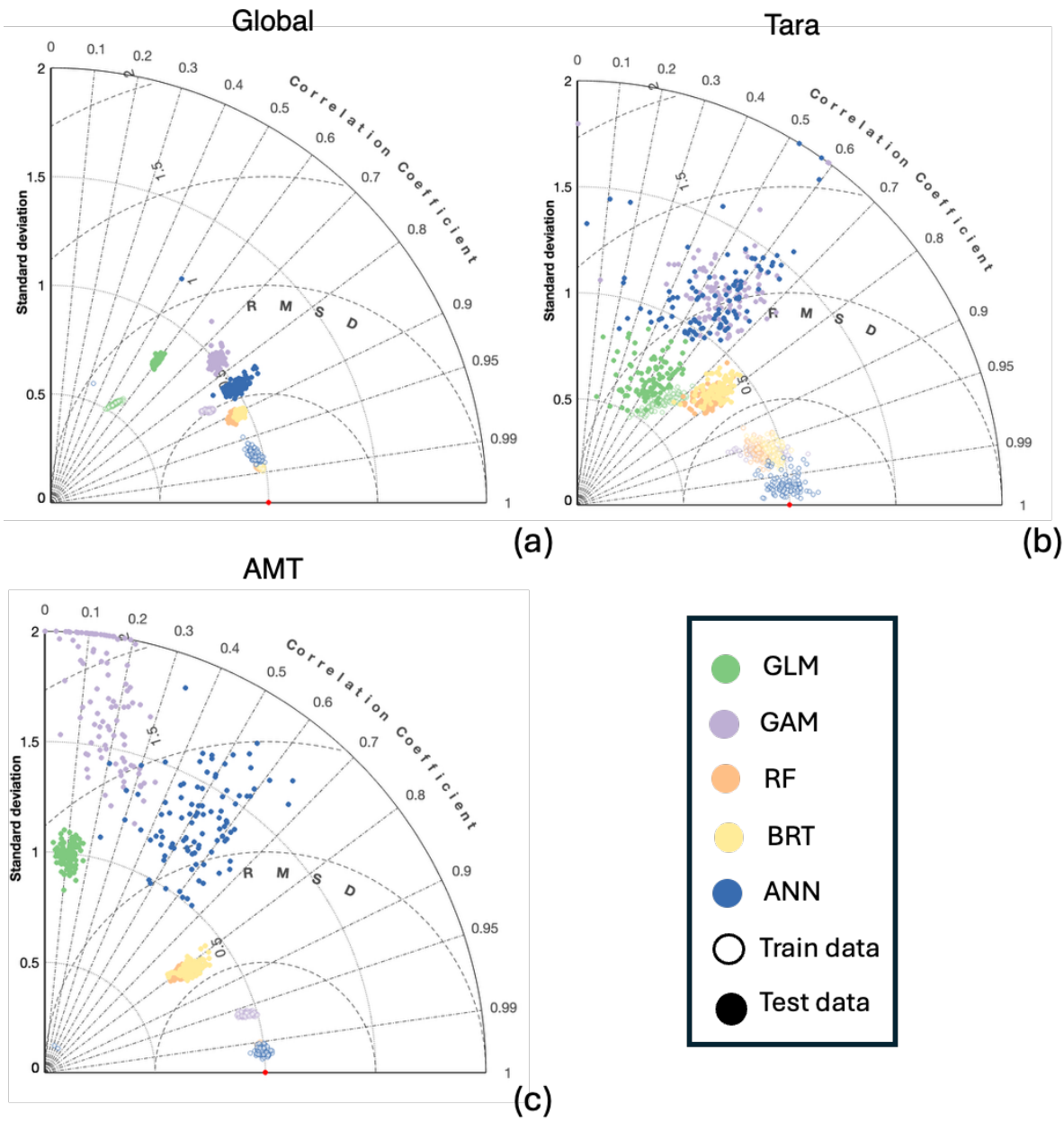

Figure 2: Model performances for 100 bootstrap runs based on the Global dataset (a), Tara Ocean dataset (b), and AMT dataset (c). Red dots represent the observation points. Empty dots represent the predictions on training datasets and the solid dots represent the predictions on test datasets. In this case, the standard deviations have been normalized by dividing them by the standard deviations of the observations. Please note that the standard deviation axis has been limited to a range of 0-2 to better visualize the main cluster of results. The full, unzoomed

version of this figure showing all data points is available in the supplementary material (Fig. S4).

3.2 Spatial distribution of errors

Although BRT and RF showed similar performance, we selected RF for subsequent in-depth analysis due to its simpler structure and its prevalence in the ecological modeling literature. With the RF model offering the best compromise in skill with regard to the picoeukaryote training and test data, we next investigated the global distribution of errors associated with the three training datasets for this SDM. This can highlight specific regional strengths and weaknesses, giving insights to point out the areas requiring further refinement and adjustment.

Mismatches between the RF model and the present and future global test data are shown in Figure 3. Errors in the present prediction based on the global dataset were predominantly distributed in areas with highly varying environment conditions, such as underestimation in high latitude area and overestimation in coastal regions (Fig. 3a). The residuals for future predictions (Fig. 3d) are significantly larger compared to the present. Areas with high error in the future predictions also extend to subtropical gyres and the Indian Ocean, where picoplankton biomass is underestimated. Predictions in polar regions switch from underestimates to overestimates in the future ocean. The residual maps clearly show that predictions based on the Tara Oceans dataset (Fig. 3c&f) perform poorly in high-latitude areas compared to those derived from the Global datasets (Fig. 3a&d), highlighting the importance of latitudinal ranges in enhancing the accuracy of predictive models. In contrast, the model trained on AMT data shows weaker performance in the Pacific and Indian oceans Fig. 3b&e). This suggests that variations observed in the Atlantic Ocean do not adequately explain conditions in the Pacific and Indian oceans. While the AMT dataset performs relatively well in representing present-day conditions in the Atlantic Ocean, its predictive skill declines

significantly when applied to future Atlantic conditions. This highlights the potential limitations of SDMs trained on current environmental data when extrapolating to future scenarios, even within the same ocean basin.

These spatial error patterns were examined for all seven plankton functional types (PFTs), with the complete residual maps provided in the supplementary material (Fig. S12–S14). While the specific regions of highest error for each PFT were closely linked to their own distinct biogeographical distributions, a consistent set of overarching patterns emerged across all functional groups. Models trained on the comprehensive Global dataset consistently produced the lowest overall prediction error (Fig. S12). In contrast, models trained on the longitudinally-biased AMT dataset reliably performed best within the Atlantic Ocean but showed substantial errors across the Pacific and Indian Oceans (Fig. S13). Finally, errors from the Tara-trained models were consistently concentrated in the under-sampled high-latitude regions (Fig. S14). This demonstrates that the spatial signature of the sampling bias in the training data is the primary driver of regional prediction error, a pattern that holds true across all functional groups.

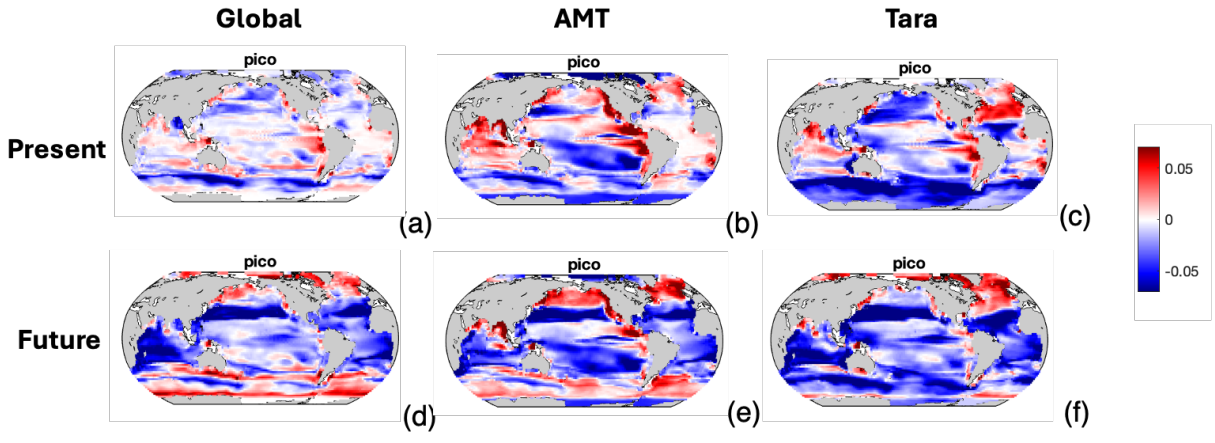

Figure 3: Residual map (µM) of biomass predictions for the RF models trained on Global datasets, AMT datasets, and Tara datasets in the present (a-c) and future (d-f) ocean. The linear

color scale represents the residual in biomass (μM) and this range corresponds to the 95% confidence interval of the residual values.

3.3 Functional groups

We can also investigate the performance of the RF model across all seven functional groups for the present and future oceans. Figure 4 presents three panels of Taylor diagrams comparing the RF model predictions against present and future test data. The Global dataset (Fig. 4a) exhibits the highest predictive skill across all PFTs, with predictions closely clustered around high correlation values and normalized standard deviations near 1. In contrast, the AMT and Tara datasets show more variable predictions, indicating reduced model accuracy. Specifically, in the AMT dataset, both diazotrophs and zooplankton exhibit the poorest performance, with low correlation coefficients and higher variance, especially in the future scenario (Fig. 4c). Similarly, the Tara dataset shows a significant decline in the predictive accuracy for diatoms (Fig. 4b). The overall performance suggests that the Global dataset provides more reliable predictions, while the AMT and Tara datasets, characterized by narrower spatiotemporal ranges, result in less reliable predictions, particularly for endemic PFTs such as diazotrophs and diatoms.

Across all three datasets, the future predictions (end of the arrows) tend to show lower accuracy compared to present predictions (start of the arrows), particularly for the AMT and Tara datasets (Fig. 4). This indicates increasing uncertainty or difficulty in modelling future scenarios with spatiotemporally incomplete datasets. However, an exception to this trend is seen with diatoms in the Tara dataset, where the future predictions are better than the present predictions.

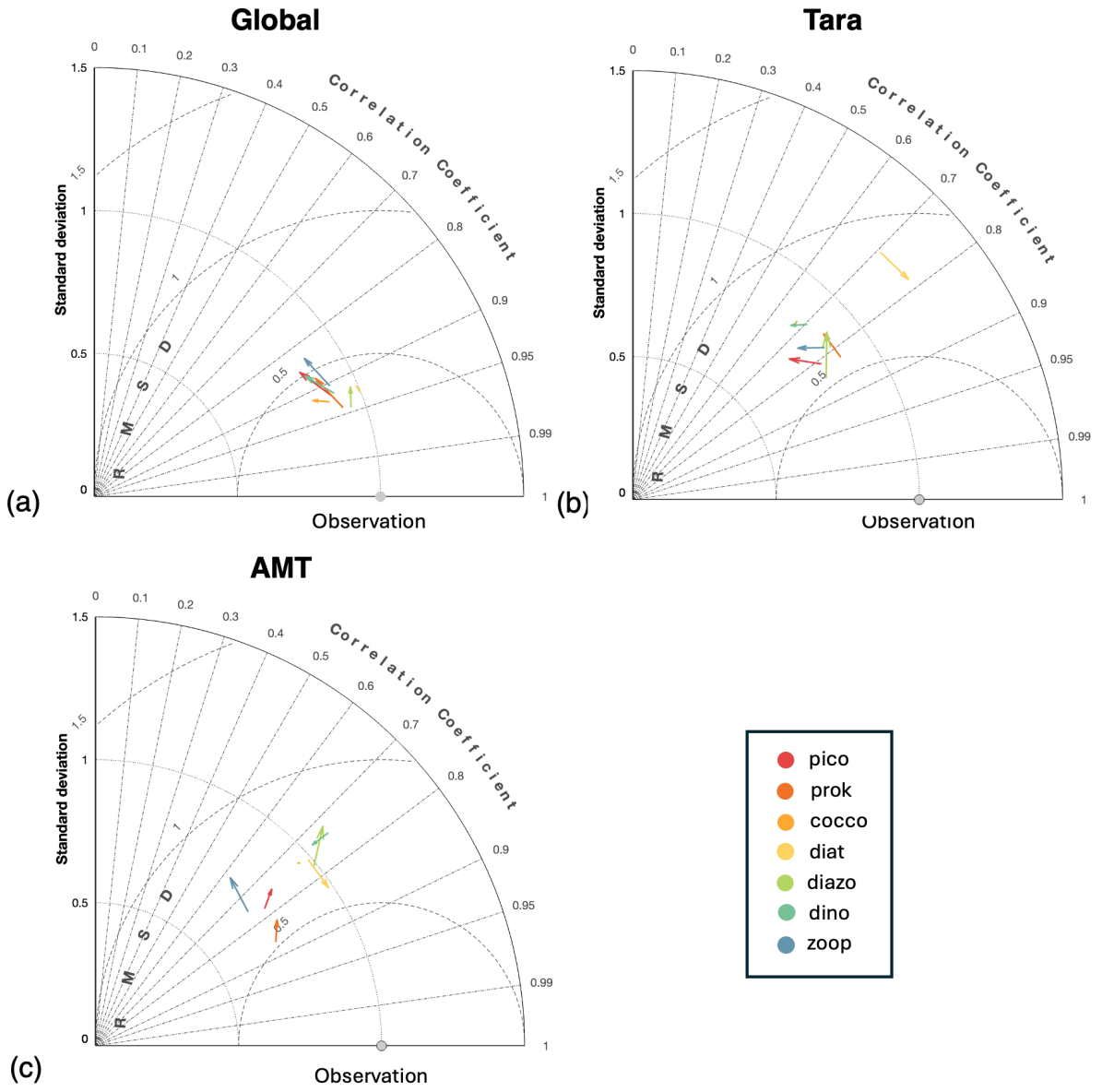

Figure 4: Performance of RF predictions based on observations of Global datasets (a), Tara datasets (b) and AMT datasets (c). Grey dots represent observation points. The starts of arrows represent the present predictions and the ends of arrows represent the future predictions. In this case, the standard deviations have been normalized by dividing them by the standard deviations of the observed biomass of different phytoplankton functional types.

3.4 Intra- and inter-annual coverage

Two further experiments were designed to investigate how monthly and yearly repeated sampling in Tara Ocean projects might improve predictions (Tara-12months, Tara-12yrs, Table 1). Our finding indicates that, within our specific experimental design, increasing the representation of intra-annual (monthly) variations in the training data was more effective at improving model performance than adding sparse inter-annual (yearly) data for most PFTs (Fig. 5).

This conclusion is specific to the nature of our experimental data: Our Tara-12yrs experiment tested the effect of adding many years of sparse (once-a-year) data. A different type of dataset, for example, one containing many years of dense, fully-resolved seasonal data, might allow an SDM to perform much better at identifying long-term trends. Nevertheless, our results clearly demonstrate that for a sampling scheme with a spatial bias like Tara, investing effort in resolving the full seasonal cycle provides a greater immediate performance benefit than repeated, sparse sampling across many years. A notable exception to this was zooplankton, where incorporating the limited inter-annual data proved more useful, perhaps reflecting their longer lifecycles and different trophic position.

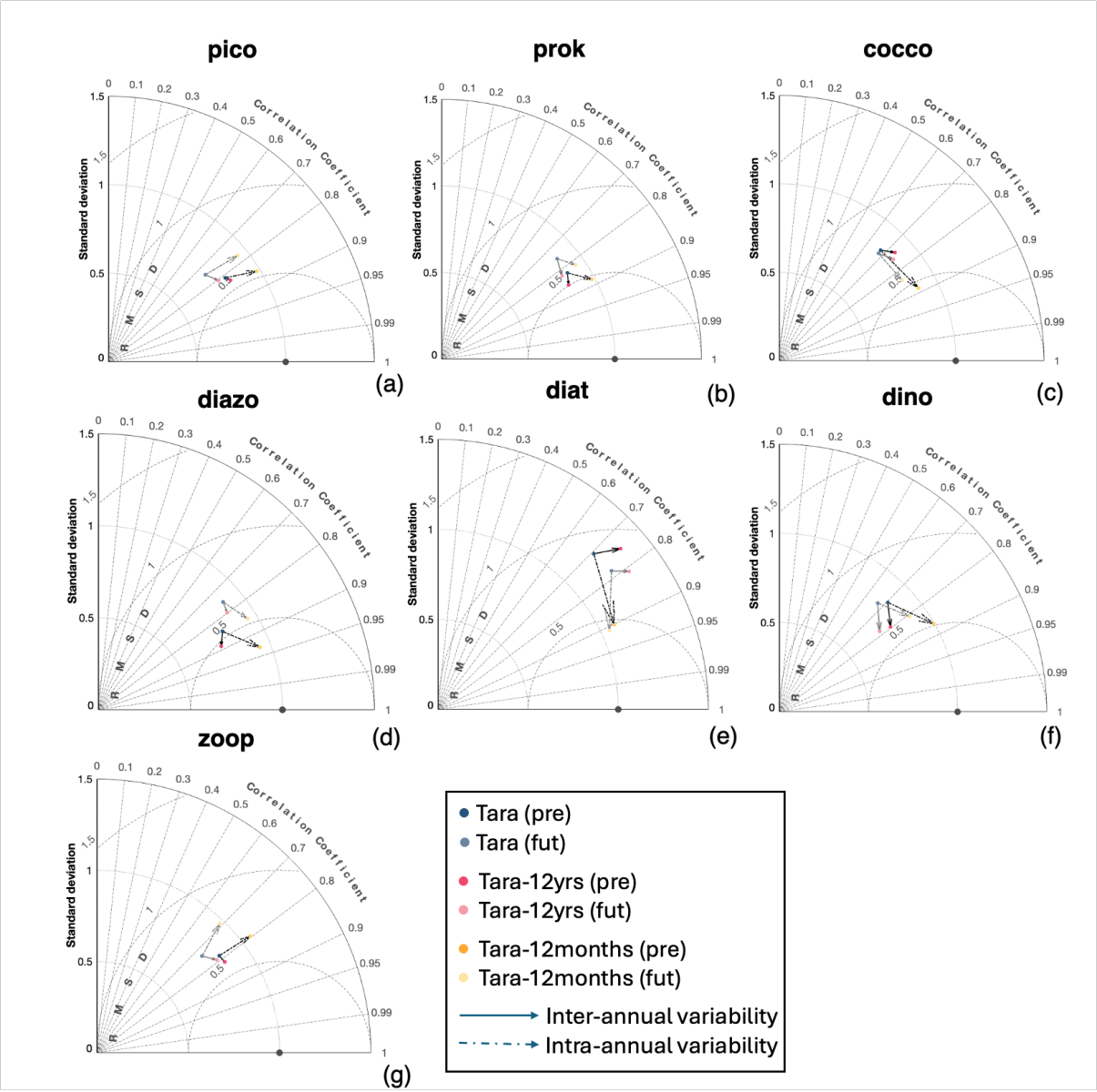

Figure 5: Performance of RF predictions for seven PFTs (a-g) based on observations of Tara Ocean (blue), Tara-12yrs (red) and Tara-12months (yellow). Grey points represent the observation points. The starts of arrows represent the original datasets and the ends of arrows represent the experimental datasets. In this case, the standard deviations have been normalized by dividing them by the standard deviations of the observed biomass of different phytoplankton functional types.

3.5 Spatial coverage

In this section, we randomized the sampling locations of the Global and Tara datasets, ensuring that the new randomized locations occupied the same number of grid cells as in the original datasets but could occur anywhere in the global ocean. This procedure simulates an idealized sampling scenario, in which the global ocean is sampled more evenly. Compared to the original datasets, the randomized Global dataset showed a slight improvement in predictive performance across all functional types (yellow arrows in Fig. 6), suggesting that more uniform sampling can help mitigate spatial biases inherent in the original data. In contrast, the randomized Tara dataset yielded mixed responses (blue arrows in Fig. 6), with reduced performance for diazotrophs but enhanced performance for diatoms. These contrasting results imply that the spatial distribution and ecological niches of different functional types may respond differently to changes in sampling strategy.

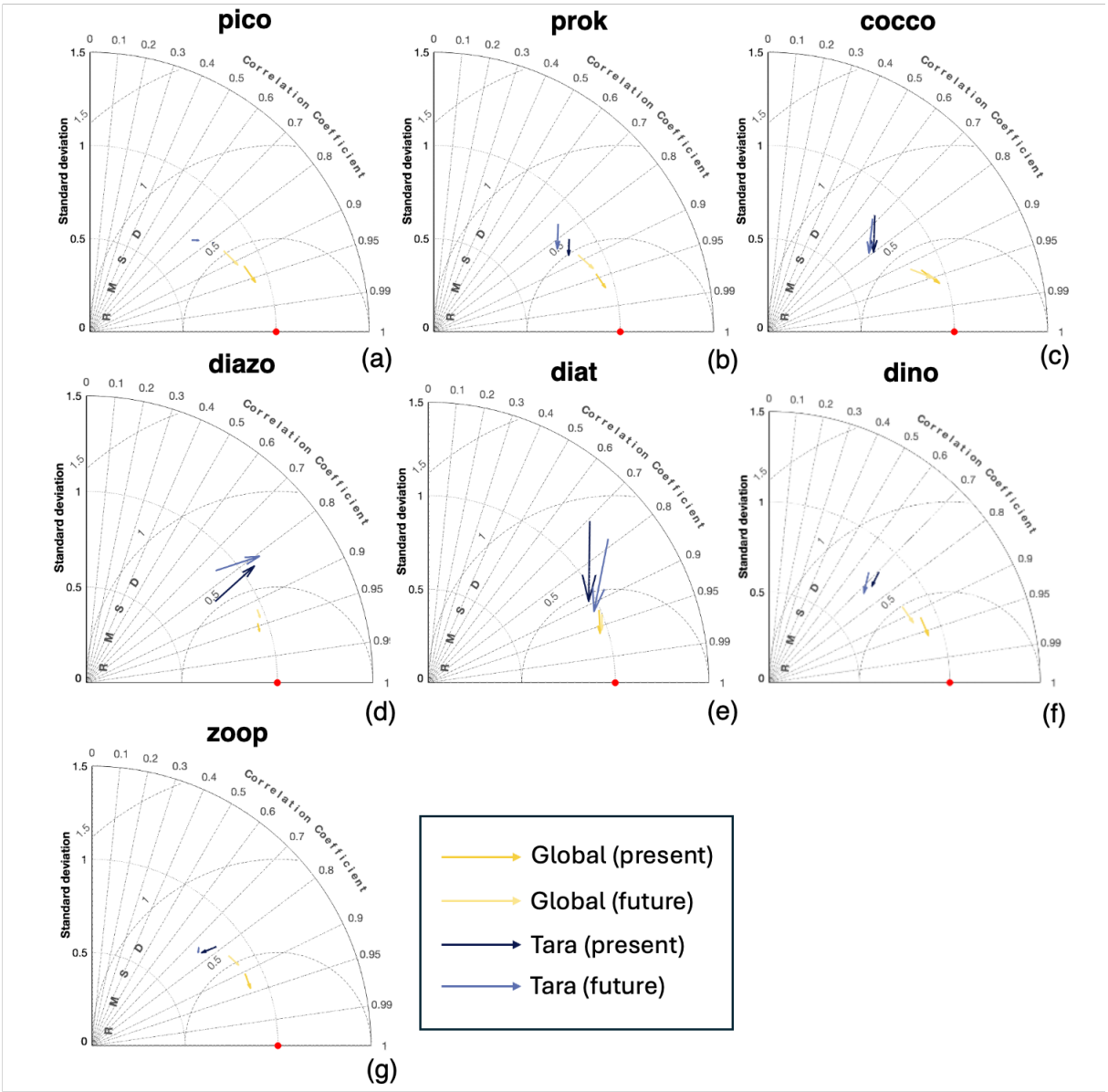

Figure 6. Taylor diagrams showing the performance of Random Forest (RF) predictions for seven plankton functional types (PFTs; a–g). Arrows start from results based on the original sampling scheme and end at those based on the idealized sampling scheme. Dark colors represent present-day predictions, while light colors indicate future projections. Blue arrows correspond to Tara datasets and yellow arrows to Global datasets. Red dots denote the reference (observations), and grey markers indicate the observation points. The standard deviations have been normalized by the standard deviations of the observed biomass of each PFT.

3.6 Sample size

To investigate whether the lower performance of the Tara and AMT-trained models was primarily due to their smaller sample sizes or their inherent spatial biases, we analyzed the results from training datasets with increased sampling density around each existing data point (Tara-densified, AMT-densified, Table 1). Our findings strongly indicate that comprehensive spatial coverage is a more critical determinant of model skill than sample size alone.

As shown in the Taylor diagram (Fig. 7), even with a nine-fold increase in sample size, the predictive skill of models trained on the AMT-densified and Tara-densified datasets still lagged considerably behind the model trained on the original Global dataset. For nearly all Plankton Functional Types (PFTs), both present and future predictions from the densified datasets exhibited lower correlation coefficients and higher RMSD compared to the Global dataset predictions.

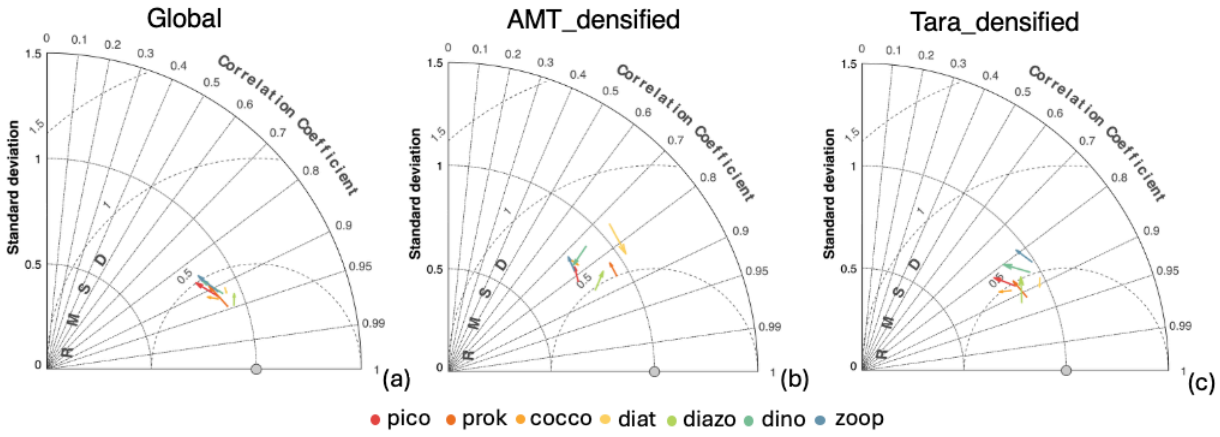

Figure 7: Taylor diagram comparing the performance of RF predictions for all PFTs. The models were trained on the original Global dataset (a), the Tara-densified dataset (b), and the AMT-densified dataset (c). The start of each arrow represents the present prediction, and the end represents the future prediction. The grey dot represents the observation point.

This conclusion is further supported by the spatial distribution of prediction errors (Fig. S15 and S16). The residual map for the AMT-densified model (Fig. S15) shows that the inherent longitudinal bias persists; prediction skill remains highest within the Atlantic Ocean, with substantial errors persisting across the Pacific and Indian Oceans. Similarly, the Tara-densified model (Fig. S16) still produces large errors in regions poorly covered by the original cruise track, particularly in the high latitudes and the eastern Pacific Ocean. These results demonstrate that simply increasing the density of samples along a spatially biased transect is insufficient to compensate for the lack of data from entire ocean basins or across critical environmental gradients.

4 Discussion

Understanding the global distribution of plankton is vital for studying biodiversity and biogeochemical cycles in the ocean, given the significant feedbacks between plankton and their environment. By focusing on realized niches of plankton, SDMs can map the abstract environmental space, defined by multiple factors, into geographic regions. However, the performance of SDMs may be influenced by various factors, leading to different levels of uncertainty in predictions. It is important to note that this study uses virtual ecosystem data, where the 'truth' is already known. This allows for a controlled assessment of SDM performance, isolating key factors contributing to uncertainty while avoiding complications arising from observational uncertainties. Our findings demonstrate that these factors include the complexity of the SDM, the temporal and spatial coverage of the data, and the relative importance of sample size versus spatial representation in overcoming sampling biases. In the following we explore these different factors with respect to the results presented above.

4.1 Model complexity and a Bias-Variance trade-off

A bias-variance trade-off is a fundamental concept in machine learning and statistics that describes the balance between two sources of error when building a model (Briscoe and Feldman, 2011). Bias error describes the error introduced when a model is too simple to capture the underlying patterns in the data. Variance error refers to the error associated with a model's sensitivity to small fluctuations in the training data. A more complex model may be able to capture more variability in the data, but this variability may include noise in the training data.

The trade-off between bias and variance generally occurs across a spectrum of model complexity, influenced by both model structure and the number of adjustable parameters (Friedman et al., 2001). Although we cannot quantify the exact complexity of each model, it is clear that the linear and additive models have significantly lower complexity compared to the machine learning models (RF, BRT, ANN). In Section 3.1, we examined the performance of five models, ranging from a very simple generalized linear model to a much more complex artificial neural network.

As one of the simplest SDMs evaluated, the GLM exhibits the least flexibility in capturing the complex relationships within the data, leading to the highest bias, particularly when predicting the training datasets. This rigid structure limits its effectiveness in dynamic marine environments. GAMs are considered to offer a middle ground, with moderate complexity and high interpretability, making them a popular choice for biogeographic predictions of plankton (Bardon et al., 2021; Righetti et al., 2019). However, in our specific case, the predictive performance of the GAM was extremely poor, especially when trained to the AMT and Tara datasets. This was likely due to its sensitivity to the spatiotemporal gaps in these datasets. Previous studies have shown that GAM can perform significantly better when applied to randomized datasets that are evenly distributed in space (Bardon et al., 2021), but our findings suggest that it struggles with the inherent biases present in real-world global datasets.

At the other end of the complexity scale, the ANN showed excellent performance when predicting the training dataset, but its significant error rates on the test data highlight high variance and overfitting issues. This suggests that although ANN may initially appear to be the best model based on its low bias error with respect to the training data, its inability to generalize well to new data brings in a very high variance error that makes it less suitable for prediction.

Finally, the two tree-based algorithms, RF and BRT, demonstrate a reliable balance between bias and variance, while both models lack the ANNs ability to precisely fit the training data. Their performance with regard to unseen test data was subject to much less variability, and thus gave more accurate predictions. The predictive skill and resilience to spatiotemporal variability of the tree-based models make them the most stable and robust choice for modelling plankton distributions in our study. Their ability to handle imbalanced datasets and avoid overfitting through ensemble methods (Breiman, 2001) further supports their utility in oceanographic modelling, where data coverage is often uneven and incomplete.

In general, our findings underscore the importance of choosing SDMs that can effectively handle spatiotemporal biases, because real-world marine datasets are rarely perfect. Tree-based models, particularly RF, provide a more reliable approach for marine SDM modelling, where the balance between skill, stability, and generality is critical.

4.2 Significance of sampling strategy on predictive SDMs

Sampling efforts can greatly influence SDM performance because predictions are sensitive to the biases present in the sampling data (Bardon et al., 2021; Inman et al., 2021; Liu et al., 2021). The AMT cruises, while spanning a wide range of latitudes, exhibit a longitudinal bias, as the transects are confined to in the Atlantic Ocean (Rees et al., 2024). In contrast, the Tara dataset samples all ocean basins, but has limited coverage at the poles, leading to a latitudinal bias

588 (Sunagawa et al., 2015). These biases are reflected in the error distribution of our SDM
589 predictions (Fig 3).

590 We also explored the SDMs' sensitivity to changing the degree of inter- and intra-annual
591 variability in the training data. While intra-annual variability is associated with seasonal
592 dynamics, inter-annual variability may be driven by longer-term trends and climatic influences.
593 While capturing inter-annual variability was not associated with the same increases in
594 predictive skill, this could occur if our data source, the Darwin model, included less inter-
595 annual variability than the real ocean, thereby making inter-annual variability less important in
596 our experiments than it may be in the real world. However, it is likely that our insights that
597 accounting for intra-annual variability leads to far greater improvement in SDM predictions of
598 plankton than inter-annual variability still broadly holds. In contrast, previous studies have
599 demonstrated that long-term variability, particularly climate-related changes, can significantly
600 enhance niche predictions by capturing ecological responses to climatic drivers (Perez-Navarro
601 et al., 2021). Studies on other marine species, such as swordfish, have shown that low-
602 frequency, long-term variability is more effective in improving predictability compared to sub-
603 annual variability (Brodie et al., 2021). This difference may stem from the fact that plankton
604 communities are often more influenced by intense seasonal (intra-annual) changes due to their
605 short lifespans and rapid turnover rates (Delong, 2012), whereas larger, longer-lived species
606 like swordfish are more sensitive to long-term climatic fluctuations.

607 Our results present a more nuanced view than the suggestion that sample size alone is
608 the most critical factor for SDM performance (e.g., Gaul et al., 2020). While the substantial
609 difference in sample size between the original Global and Tara datasets is a significant
610 confounding variable, our "densified sampling" experiment was designed to disentangle these
611 effects. In that experiment, we showed that the SDMs trained on the Tara-densified and AMT-
612 densified datasets still performed significantly worse than when trained on the Global dataset,

even though they contained a similar number of samples. This demonstrates that merely increasing the density of samples along a spatially biased transect is insufficient to overcome the limitations imposed by poor spatial coverage. Therefore, we conclude that sampling strategy, achieving broad spatial and environmental coverage, is a more critical determinant of SDM performance than sample size alone.

4.3 Different SDM performance on functional types in SDMs

Understanding the predictive capabilities for different PFTs is crucial for evaluating the feasibility and reliability of SDMs in real-world applications. By examining the impacts of sampling biases on PFTs with distinct habitat preferences, we can better assess whether SDMs can accurately capture species distributions under varying environmental and data conditions.

In our study, sampling bias had less influence on the prediction of cosmopolitan species like prokaryotes and pico-eukaryotes, as demonstrated by the comparable results across the three datasets (Fig. 3). The case is different for diazotrophs and diatom with endemic biomass distributions.

The Tara Ocean dataset has a latitudinal sampling bias, while the AMT dataset is longitudinally biased. This difference in sampling bias affects species differently, depending on their spatial distribution patterns. Diazotrophs, which exhibit a more longitudinal distribution pattern, are more concentrated at low latitudes with higher densities in the western Pacific and Atlantic Oceans and lower densities in eastern regions, likely influenced by the availability of iron and phosphate (Shao et al., 2023). In contrast, diatoms follow a latitudinal distribution pattern; they are most abundant in nutrient-rich areas at high latitudes, and accurate predictions for diatoms require sampling that spans a wide latitudinal range with varying nutrient levels (Malviya et al., 2016).

Our results from the randomized datasets clearly illustrate these contrasting patterns. For diatoms, which thrive in nutrient-rich high latitudes, the original Tara dataset performed poorly due to its under-sampling of polar regions (latitudinal bias). Consequently, when we applied the randomized Tara sampling scheme, which uniformly covers all latitudes, diatom predictions improved significantly (Fig. 6e). In contrast, the randomized-Tara sampling shows no improvements in prediction accuracy for diazotrophs. Since diazotrophs are primarily restricted to low-latitude warm waters, the original Tara dataset's concentration in these regions captured their core habitat well. These findings underscore that the impact of sampling bias is not uniform, it depends critically on whether the bias matches or misses the species' ecological niche.

4.4 Present and future prediction

Comparing accuracy of SDMs for present day and future predictions is crucial for understanding the robustness of SDMs under changing environmental conditions. In our study, the future prediction of plankton biomass is generally worse than the present prediction of plankton biomass except for diatoms (Fig. 3). This result can be attributed to two possible reasons. On one hand, while using SDMs to predict the biogeography of plankton in the future ocean, the correlations come from the trained model based on historical data, implicitly assuming these ecological relationships remain identical in the future (Wiens et al., 2009). This can be particularly problematic if the identified predictor variables are only correlates of the plankton distributions, and not the true drivers (Bardon et al., 2021). Large errors can be introduced if these correlations change through time, especially when the future test data, compared to the present test data, diverges more significantly from the training data.

On the other hand, ocean dispersal processes, ranging from small-scale physical phenomena to large-scale ocean circulation, play a significant role in driving phytoplankton distributions (Clayton et al., 2013; Mousing et al., 2016; Yan et al., 2023). As a result, the

realized niche of plankton can expand to areas where environmental conditions or biotic interactions may not be ecologically and physiologically suitable for their growth. The dispersal effects can indeed result in the realized niche lying partially outside, rather than exclusively within the fundamental niche. However, the environmental variables we used for correlation are all attributes of the fundamental niche, so predicting environmental distributions outside the fundamental niche may be challenging for SDMs.

Consequently, variations in phytoplankton biomass cannot be fully explained by SDMs, which primarily focus on the relationships between biomass and abiotic environmental factors. Further studies are needed to explore how correlations change with climate and dispersal effects.

4.5 Limitations and future prospects

A primary consideration in interpreting our results is that we assessed SDMs using a "perfect world" model framework, where we used output from a virtual ecosystem model as a testbed rather than real-world observational data. The relationships between environmental drivers and plankton biomass within the deterministic ecosystem model are inherently cleaner and more defined than those in the complex and often noisy real ocean for which observations have myriad confounding experimental errors and uncertainties. Consequently, the absolute performance metrics (e.g., correlation coefficients, RMSD) reported here are likely optimistic and represent an upper bound on the skill that could be expected when applying these SDMs to sparse field observations. If SDMs perform poorly when assessed using model output, they are likely to perform even more poorly when applied to real-world data.

However, this approach was a deliberate and necessary choice. By using a model where the "ground truth" is perfectly known globally for present day and into the future, we were able to isolate and rigorously quantify the specific impacts of sampling bias and algorithm choice

on SDM performance. This type of controlled assessment would be impossible with limited *in situ* observational data, where the observations for validation are sparse and observational errors would confound the analysis. This is particularly the case for the ocean ecosystem analysis, where measurement techniques and uncertainties differ for different components of the ecosystem. Thus, our study provides a unique and clean evaluation of these key sources of uncertainty that are fundamental to all SDM applications.

While the relative performance ranking of the SDM algorithms and the identified impacts of sampling bias are likely robust findings, future work is needed to apply these insights to real-world plankton datasets. Such studies will need to carefully account for the types of spatial and temporal sampling biases that we have highlighted, and ideally experimental uncertainties as well. A crucial next step will be to use the lessons learned from this controlled experiment to better constrain and interpret SDMs applied to the challenge of predicting real-world plankton biogeography, thereby bridging the gap between theoretical model performance and practical applications.

5 Comments and recommendations

This study compared the potential of several SDMs to predict plankton biogeography and found that tree-based algorithms are the best choices for reliable performance against both test and training data from virtual ecosystem where the truth was already known. A 'bias-variance' trade-off in model selection became apparent with more spatially incomplete training data. We tested three different spatially and temporally biased datasets and highlighted the significant impact of these biases on model performance. Models trained with less spatially-biased datasets yielded more accurate predictions than those trained with more biased datasets. Our analysis also underscored the importance of including higher temporal resolved observations also significantly improved model robustness. We showed how the choice of sampling locations

709 influences model performance, especially for widely distributed vs endemic PFTs. Overall, our
710 findings underscore that it is necessary to consider sampling strategies and model choice in
711 predicting plankton biogeography. Further research could be done to test how the uncertainty
712 and assumptions of SDMs, including dispersal limitations and extrapolation in future
713 prediction, will influence their predictive skills.

Acknowledgments

ZS was funded by the University of Southampton INSPIRE DTP studentship and the Royal Society. BAW was funded by the Royal Society and the BIOcean5D program. BC and TP were funded by the BIOcean5D program. S.D acknowledges funding from the Simons Collaboration on Computational Biogeochemical Modeling of Marine Ecosystem/CBIOMES (grant 549931). This research was co-Funded by the European Union. Views and opinions expressed are however those of the authors only and do not necessarily reflect those of the European Union. Neither the European Union nor the granting authority can be held responsible for them.

Data Availability Statement

The physical model used in the Darwin simulation is the MIT General Circulation Model (MITgcm), accessible at http://mitgcm.org. The generic ecosystem code is available at https://gitlab.com/jahn/gud, and detailed equations and documentation can be found at https://darwin3.readthedocs.io/en/latest/phys_pkgs/darwin.html. The Darwin model data can be downloaded at https://doi.org/10.7910/DVN/RPL6PT and https://doi.org/10.7910/DVN/LQH9PX. The SDMs model script can be accessed in GitHub https://github.com/ZhiboShao/uncertainty-and-predicitability-of-plankton-SDM-. The data can be found in Zenodo https://doi.org/10.5281/zenodo.14219377 .

Reference

Baert, J. M., De Laender, F., Sabbe, K., & Janssen, C. R. (2016). Biodiversity increases functional and compositional resistance, but decreases resilience in phytoplankton communities. *Ecology*, *97*(12), 3433-3440. https://doi.org/https://doi.org/10.1002/ecy.1601

Ban, Z., Hu, X., & Li, J. (2022). Tipping points of marine phytoplankton to multiple environmental stressors. *Nature Climate Change*, *12*(11), 1045-1051. https://doi.org/10.1038/s41558-022-01489-0

Bardon, L. R., Ward, B. A., Dutkiewicz, S., & Cael, B. B. (2021). Testing the Skill of a Species Distribution Model Using a 21st Century Virtual Ecosystem. *Geophysical Research Letters*, *48*(22), e2021GL093455. https://doi.org/https://doi.org/10.1029/2021GL093455

Barton, A. D., Irwin, A. J., Finkel, Z. V., & Stock, C. A. (2016). Anthropogenic climate change drives shift and shuffle in North Atlantic phytoplankton communities. *Proceedings of the National Academy of Sciences*, *113*(11), 2964-2969. https://doi.org/doi:10.1073/pnas.1519080113

Benedetti, F., Vogt, M., Elizondo, U. H., Righetti, D., Zimmermann, N. E., & Gruber, N. (2021). Major restructuring of marine plankton assemblages under global warming. *Nature Communications*, *12*(1), 5226. https://doi.org/10.1038/s41467-021-25385-x

Bourel, M., Crisci, C., & Martínez, A. (2017). Consensus methods based on machine learning techniques for marine phytoplankton presence–absence prediction. *Ecological Informatics*, *42*, 46-54. https://doi.org/https://doi.org/10.1016/j.ecoinf.2017.09.004

Breiman, L. (2001). Random Forests. *Machine Learning*, *45*(1), 5-32. https://doi.org/10.1023/A:1010933404324

Briscoe, E., & Feldman, J. (2011). Conceptual complexity and the bias/variance tradeoff. *Cognition*, *118*(1), 2-16. https://doi.org/https://doi.org/10.1016/j.cognition.2010.10.004

Brodie, S., Abrahms, B., Bograd, S. J., Carroll, G., Hazen, E. L., Muhling, B. A., Pozo Buil, M., Smith, J. A., Welch, H., & Jacox, M. G. (2021). Exploring timescales of predictability in species distributions. *Ecography*, *44*(6), 832-844. https://doi.org/https://doi.org/10.1111/ecog.05504

Brun, P., Kiørboe, T., Licandro, P., & Payne, M. R. (2016). The predictive skill of species distribution models for plankton in a changing climate. *Global Change Biology*, *22*(9), 3170-3181. https://doi.org/https://doi.org/10.1111/gcb.13274

Cael, B. B., Dutkiewicz, S., & Henson, S. (2021). Abrupt shifts in 21st-century plankton communities. *Science Advances*, *7*(44), eabf8593. https://doi.org/doi:10.1126/sciadv.abf8593

Chen, B., Liu, H., Xiao, W., Wang, L., & Huang, B. (2020). A machine-learning approach to modeling picophytoplankton abundances in the South China Sea. *Progress in Oceanography*, *189*, 102456. https://doi.org/https://doi.org/10.1016/j.pocean.2020.102456

Clayton, S., Dutkiewicz, S., Jahn, O., & Follows, M. J. (2013). Dispersal, eddies, and the diversity of marine phytoplankton. *Limnology and Oceanography: Fluids and Environments*, *3*(1), 182-197. https://doi.org/https://doi.org/10.1215/21573689-2373515

DeLong, E. F. (2012). Microbial Evolution in the Wild. *Science*, *336*(6080), 422-424. https://doi.org/doi:10.1126/science.1221822

Dutkiewicz, S., Boyd, P. W., & Riebesell, U. (2021). Exploring biogeochemical and ecological redundancy in phytoplankton communities in the global ocean. *Global Change Biology*, *27*(6), 1196-1213. https://doi.org/https://doi.org/10.1111/gcb.15493

Elith, J., & Franklin, J. (2017). Species Distribution Modeling. In *Reference Module in Life Sciences*. Elsevier. https://www.sciencedirect.com/science/article/pii/B9780128096338023906

Elith, J., Leathwick, J. R., & Hastie, T. (2008). A working guide to boosted regression trees. *Journal of Animal Ecology*, *77*(4), 802-813. https://doi.org/https://doi.org/10.1111/j.1365-2656.2008.01390.x

Flombaum, P., Gallegos, J. L., Gordillo, R. A., Rincón, J., Zabala, L. L., Jiao, N., Karl, D. M., Li, W. K. W., Lomas, M. W., Veneziano, D., Vera, C. S., Vrugt, J. A., & Martiny, A. C. (2013). Present and future global distributions of the marine Cyanobacteria *Prochlorococcus* and *Synechococcus*. *Proceedings of the National Academy of Sciences*, *110*(24), 9824-9829. https://doi.org/doi:10.1073/pnas.1307701110

Flombaum, P., Wang, W.-L., Primeau, F. W., & Martiny, A. C. (2020). Global picophytoplankton niche partitioning predicts overall positive response to ocean warming. *Nature Geoscience*, *13*(2), 116-120. https://doi.org/10.1038/s41561-019-0524-2

Frémont, P., Gehlen, M., & Jaillon, O. (2023). Plankton biogeography in the 21st century and impacts of climate change: advances through genomics. *Comptes Rendus. Biologies*, *346*, 13-24. https://doi.org/10.5802/crbiol.107

Frémont, P., Gehlen, M., Vrac, M., Leconte, J., Delmont, T. O., Wincker, P., Iudicone, D., & Jaillon, O. (2022). Restructuring of plankton genomic biogeography in the surface ocean under climate change. *Nature Climate Change*, *12*(4), 393-401. https://doi.org/10.1038/s41558-022-01314-8

Friedman, J., Hastie, T., & Tibshirani, R. (2001). The elements of statistical learning. vol. 1 Springer series in statistics. *New York*.

Gattuso, J.-P., Frankignoulle, M., & Wollast, R. (1998). CARBON AND CARBONATE METABOLISM IN COASTAL AQUATIC ECOSYSTEMS. *Annual Review of Ecology, Evolution, and Systematics*, *29*(Volume 29, 1998), 405-434. https://doi.org/https://doi.org/10.1146/annurev.ecolsys.29.1.405

Guillera-Arroita, G., Lahoz-Monfort, J. J., Elith, J., Gordon, A., Kujala, H., Lentini, P. E., McCarthy, M. A., Tingley, R., & Wintle, B. A. (2015). Is my species distribution model fit for purpose? Matching data and models to applications [Review]. *Global Ecology and Biogeography*, *24*(3), 276-292. https://doi.org/10.1111/geb.12268

Hastie, T. J. (1990). Generalized additive models. In *Statistical models in S* (pp. 249-307). Routledge.

Henson, S. A., Cael, B. B., Allen, S. R., & Dutkiewicz, S. (2021). Future phytoplankton diversity in a changing climate. *Nature Communications*, *12*(1), 5372. https://doi.org/10.1038/s41467-021-25699-w

Hernandez, P. A., Graham, C. H., Master, L. L., & Albert, D. L. (2006). The Effect of Sample Size and Species Characteristics on Performance of Different Species Distribution Modeling Methods. *Ecography*, *29*(5), 773-785. http://www.jstor.org/stable/30243167

Hornik, K., Stinchcombe, M., & White, H. (1989). Multilayer feedforward networks are universal approximators. *Neural Networks*, *2*(5), 359-366. https://doi.org/https://doi.org/10.1016/0893-6080(89)90020-8

Hughes, A. C., Orr, M. C., Ma, K., Costello, M. J., Waller, J., Provoost, P., Yang, Q., Zhu, C., & Qiao, H. (2021). Sampling biases shape our view of the natural world. *Ecography*, *44*(9), 1259-1269. https://doi.org/https://doi.org/10.1111/ecog.05926

827 Hutchinson, G. E. (1957). Concluding remarks. Cold Spring Harbor symposia on quantitative
828 biology,
829 Inman, R., Franklin, J., Esque, T., & Nussear, K. (2021). Comparing sample bias correction
830 methods for species distribution modeling using virtual species. *Ecosphere*, *12*(3),
831 e03422. https://doi.org/https://doi.org/10.1002/ecs2.3422
832 Le Quéré, C., Buitenhuis, E. T., Moriarty, R., Alvain, S., Aumont, O., Bopp, L., Chollet, S.,
833 Enright, C., Franklin, D. J., Geider, R. J., Harrison, S. P., Hirst, A. G., Larsen, S.,
834 Legendre, L., Platt, T., Prentice, I. C., Rivkin, R. B., Sailley, S., Sathyendranath,
835 S., . . . Vallina, S. M. (2016). Role of zooplankton dynamics for Southern Ocean
836 phytoplankton biomass and global biogeochemical cycles. *Biogeosciences*, *13*(14),
837 4111-4133. https://doi.org/10.5194/bg-13-4111-2016
838 Litchman, E., de Tezanos Pinto, P., Edwards, K. F., Klausmeier, C. A., Kremer, C. T., &
839 Thomas, M. K. (2015). Global biogeochemical impacts of phytoplankton: a trait-
840 based perspective. *Journal of Ecology*, *103*(6), 1384-1396.
841 https://doi.org/https://doi.org/10.1111/1365-2745.12438
842 Liu, W., Ikonnikova, S., Scott Hamlin, H., Sivila, L., & Pyrcz, M. J. (2021). Demonstration
843 and Mitigation of Spatial Sampling Bias for Machine-Learning Predictions. *SPE*
844 *Reservoir Evaluation & Engineering*, *24*(01), 262-274.
845 https://doi.org/10.2118/203838-pa
846 Malviya, S., Scalco, E., Audic, S., Vincent, F., Veluchamy, A., Poulain, J., Wincker, P.,
847 Iudicone, D., de Vargas, C., Bittner, L., Zingone, A., & Bowler, C. (2016). Insights
848 into global diatom distribution and diversity in the world's ocean. *Proceedings of the*
849 *National Academy of Sciences*, *113*(11), E1516-E1525.
850 https://doi.org/doi:10.1073/pnas.1509523113
851 Marshall, J., Adcroft, A., Hill, C., Perelman, L., & Heisey, C. (1997). A finite-volume,
852 incompressible Navier Stokes model for studies of the ocean on parallel computers.
853 *Journal of Geophysical Research: Oceans*, *102*(C3), 5753-5766.
854 https://doi.org/https://doi.org/10.1029/96JC02775
855 McCullagh, P. (1989). *Generalized linear models*. Routledge.
856 https://doi.org/https://doi.org/10.1201/9780203753736
857 Melo-Merino, S. M., Reyes-Bonilla, H., & Lira-Noriega, A. (2020). Ecological niche models
858 and species distribution models in marine environments: A literature review and
859 spatial analysis of evidence. *Ecological Modelling*, *415*, 108837.
860 https://doi.org/https://doi.org/10.1016/j.ecolmodel.2019.108837
861 Monier, E., Paltsev, S., Sokolov, A., Chen, Y. H. H., Gao, X., Ejaz, Q., Couzo, E., Schlosser,
862 C. A., Dutkiewicz, S., Fant, C., Scott, J., Kicklighter, D., Morris, J., Jacoby, H., Prinn,
863 R., & Haigh, M. (2018). Toward a consistent modeling framework to assess multi-
864 sectoral climate impacts. *Nature Communications*, *9*(1), 660.
865 https://doi.org/10.1038/s41467-018-02984-9
866 Mousing, E. A., Richardson, K., Bendtsen, J., Cetinić, I., & Perry, M. J. (2016). Evidence of
867 small-scale spatial structuring of phytoplankton alpha- and beta-diversity in the open
868 ocean. *Journal of Ecology*, *104*(6), 1682-1695.
869 https://doi.org/https://doi.org/10.1111/1365-2745.12634
870 O'Brien, C. J., Peloquin, J. A., Vogt, M., Heinle, M., Gruber, N., Ajani, P., Andruleit, H.,
871 Arístegui, J., Beaufort, L., Estrada, M., Karentz, D., Kopczyńska, E., Lee, R., Poulton,
872 A. J., Pritchard, T., & Widdicombe, C. (2013). Global marine plankton functional type
873 biomass distributions: coccolithophores. *Earth Syst. Sci. Data*, *5*(2), 259-276.
874 https://doi.org/10.5194/essd-5-259-2013
875 Perez-Navarro, M. A., Broennimann, O., Esteve, M. A., Moya-Perez, J. M., Carreño, M. F.,
876 Guisan, A., & Lloret, F. (2021). Temporal variability is key to modelling the climatic

niche. *Diversity and Distributions*, *27*(3), 473-484. https://doi.org/https://doi.org/10.1111/ddi.13207
Pinkerton, M. H., Smith, A. N. H., Raymond, B., Hosie, G. W., Sharp, B., Leathwick, J. R., & Bradford-Grieve, J. M. (2010). Spatial and seasonal distribution of adult Oithona similis in the Southern Ocean: Predictions using boosted regression trees. *Deep Sea Research Part I: Oceanographic Research Papers*, *57*(4), 469-485. https://doi.org/https://doi.org/10.1016/j.dsr.2009.12.010
Rees, A. P., Smyth, T. J., & Brotas, V. (2024). Editorial: The Atlantic Meridional Transect programme (1995-2023) [Editorial]. *Frontiers in Marine Science*, *11*. https://doi.org/10.3389/fmars.2024.1358174
Riahi, K., Rao, S., Krey, V., Cho, C., Chirkov, V., Fischer, G., Kindermann, G., Nakicenovic, N., & Rafaj, P. (2011). RCP 8.5—A scenario of comparatively high greenhouse gas emissions. *Climatic Change*, *109*(1), 33. https://doi.org/10.1007/s10584-011-0149-y
Righetti, D., Vogt, M., Gruber, N., Psomas, A., & Zimmermann, N. E. (2019). Global pattern of phytoplankton diversity driven by temperature and environmental variability. *Science Advances*, *5*(5), eaau6253. https://doi.org/doi:10.1126/sciadv.aau6253
Robinson, N. M., Nelson, W. A., Costello, M. J., Sutherland, J. E., & Lundquist, C. J. (2017). A Systematic Review of Marine-Based Species Distribution Models (SDMs) with Recommendations for Best Practice [Systematic Review]. *Frontiers in Marine Science*, *4*. https://doi.org/10.3389/fmars.2017.00421
Shao, Z., Xu, Y., Wang, H., Luo, W., Wang, L., Huang, Y., Agawin, N. S. R., Ahmed, A., Benavides, M., Bentzon-Tilia, M., Berman-Frank, I., Berthelot, H., Biegala, I. C., Bif, M. B., Bode, A., Bonnet, S., Bronk, D. A., Brown, M. V., Campbell, L., . . . Luo, Y. W. (2023). Global oceanic diazotroph database version 2 and elevated estimate of global oceanic N2 fixation. *Earth Syst. Sci. Data*, *15*(8), 3673-3709. https://doi.org/10.5194/essd-15-3673-2023
Simpson, J. H., & Sharples, J. (2012). *Introduction to the physical and biological oceanography of shelf seas*. Cambridge University Press.
Sunagawa, S., Coelho, L. P., Chaffron, S., Kultima, J. R., Labadie, K., Salazar, G., Djahanschiri, B., Zeller, G., Mende, D. R., Alberti, A., Cornejo-Castillo, F. M., Costea, P. I., Cruaud, C., d'Ovidio, F., Engelen, S., Ferrera, I., Gasol, J. M., Guidi, L., Hildebrand, F., . . . Velayoudon, D. (2015). Structure and function of the global ocean microbiome. *Science*, *348*(6237), 1261359. https://doi.org/doi:10.1126/science.1261359
Tang, W., & Cassar, N. (2019). Data-Driven Modeling of the Distribution of Diazotrophs in the Global Ocean. *Geophysical Research Letters*, *46*(21), 12258-12269. https://doi.org/https://doi.org/10.1029/2019GL084376
Taylor, K. E. (2001). Summarizing multiple aspects of model performance in a single diagram. *Journal of Geophysical Research: Atmospheres*, *106*(D7), 7183-7192. https://doi.org/https://doi.org/10.1029/2000JD900719
Villarino, E., Chust, G., Licandro, P., Butenschön, M., Ibaibarriaga, L., Larrañaga, A., & Irigoien, X. (2015). Modelling the future biogeography of North Atlantic zooplankton communities in response to climate change. *Marine Ecology Progress Series*, *531*, 121-142. https://www.int-res.com/abstracts/meps/v531/p121-142
Wiens, J. A., Stralberg, D., Jongsomjit, D., Howell, C. A., & Snyder, M. A. (2009). Niches, models, and climate change: Assessing the assumptions and uncertainties. *Proceedings of the National Academy of Sciences*, *106*(supplement_2), 19729-19736. https://doi.org/doi:10.1073/pnas.0901639106
Yan, Z.-G., Zhu, X.-M., Zhang, S.-W., Jiang, H., Wang, S.-P., Wei, C., Wang, J., Shao, Y., Liu, C., & Wang, H. (2023). Environmental DNA sequencing reveals the regional

difference in diversity and community assembly mechanisms of eukaryotic plankton in coastal waters [Original Research]. *Frontiers in Microbiology*, *14*. https://doi.org/10.3389/fmicb.2023.1132925

Supplementary

Methods

In this study, a variety of statistical and machine learning methods were employed to model species distributions. Specifically, for Species Distribution Models (SDMs), Generalized Linear Models (GLMs), Random Forest (RF), and Boosted Regression Trees (BRT), the scikit-learn (sklearn) package in Python was utilized due to its robust and efficient implementation of these algorithms (Pedregosa et al., 2011). For Generalized Additive Models (GAMs), the pyGAM package was chosen, offering a flexible framework for modeling complex, non-linear relationships. Additionally, for constructing Artificial Neural Networks (ANNs), PyTorch was used.

The GLM assumes linear relationships between predictors and outcomes, providing straightforward interpretation but limited flexibility for complex patterns. While the GAM allows for nonlinear relationships, making it better suited for ecological data with curved trends. The RF is a decision-tree ensemble that builds multiple trees using randomly selected subsets of data and predictors, and then averages their predictions. This approach improves accuracy and provides insights into feature importance while reducing overfitting. The BRT is also a decision tree ensemble that refines predictions iteratively, enhancing model performance and interpretability by focusing on harder-to-predict cases. The ANN used here is a multilayer perceptron (MLP), which can capture complex, high-dimensional relationships in the data, making it suitable for intricate ecological patterns. However, due to its layered structure, MLPs can be more challenging to interpret compared to other models.

For species distribution models, RF, BRT, ANN, in which hyperparameters (Table S1) had to be optimised, we performed a N-fold cross-validation procedure to determine the best combinations (Fig S1). In this process, the training data were equally divided into N subsets, or folds. At each iteration, one fold served as a validation set, while the remaining folds served as the training set. In each cross-validation, only one model type was trained. N of these models were trained, where N is the number of folds.

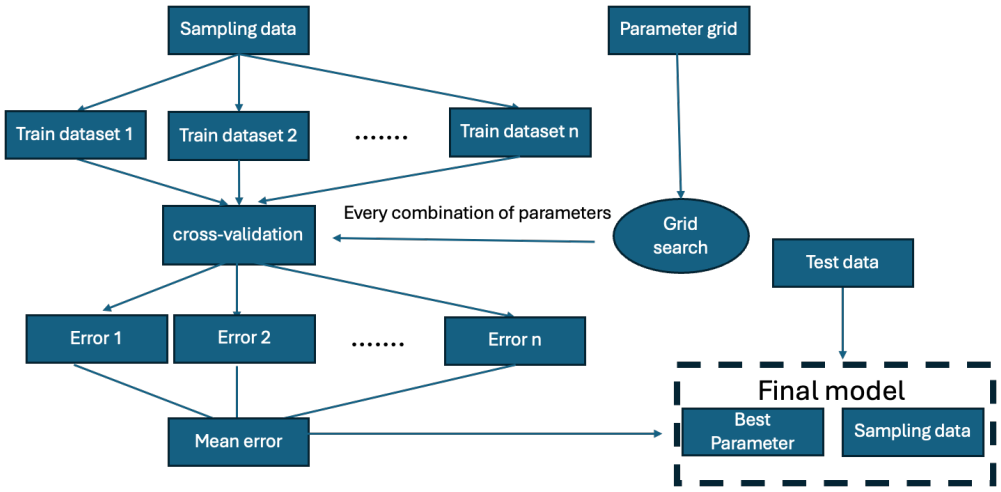

Figure S1: Flow chart of cross-validation in model training.

The performance results from all validation sets are then averaged to produce the final model's performance. Based on these averaged performance metrics, we select the optimal hyperparameters for the model. We tried five experiments for the number of CV folds (N = 3, 5, 8, 10, 12) in RF, BRT and ANN. The sensitivity test demonstrates that the variance and mean error generated in the validation set did not result in significant differences in BRT and RF (Fig S2). When folds number reaches 8, error of different folds in ANN prediction stabilises. Therefore, we chose 8 as the number of CV folds in cross-validation for RF, BRT and ANN.

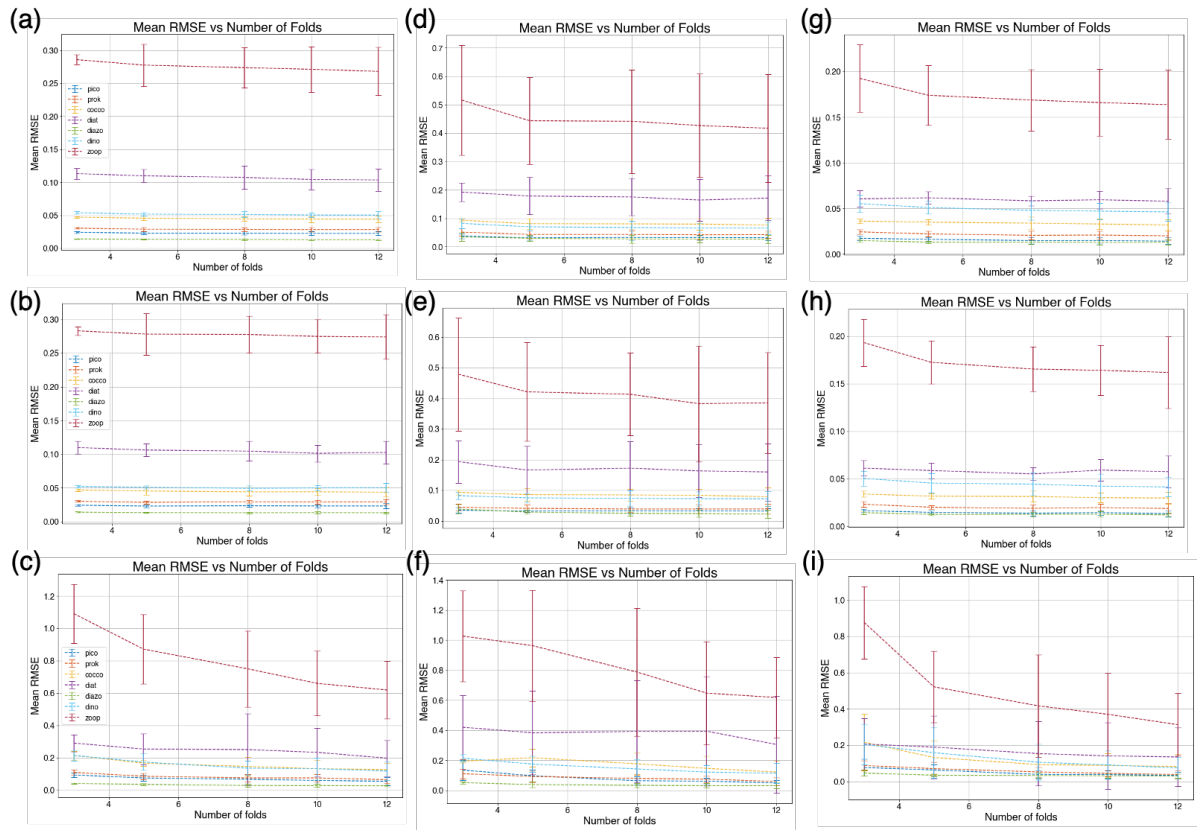

Figure S2: Sensitivity test of folds number in cross-validation of RF (a, d, g), BRT (b, e, h), ANN (c, f, i) trained by three types of datasets, the Global datasets (a-c), the Tara dataset (d-f) and the AMT dataset (g-i).

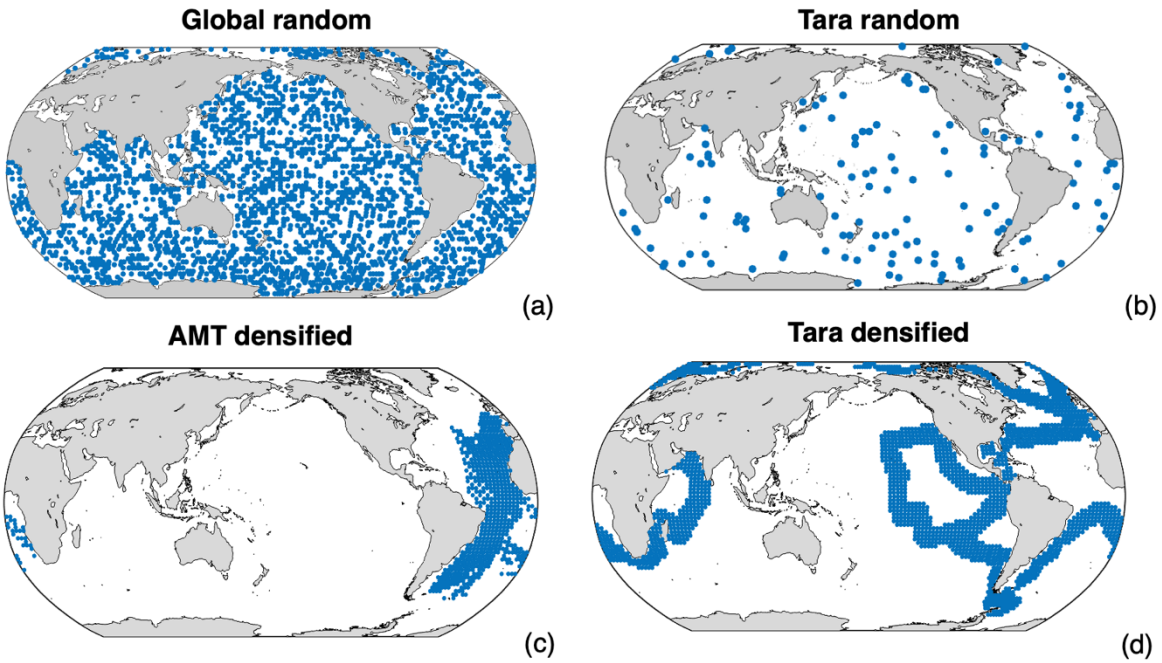

Figure S3. Sampling locations for the experimental datasets used in this study. (a) Global random *dataset, (b)* Tara random *dataset, (c)* AMT densified *dataset, and (d)* Tara densified *dataset. These spatial distributions represent the sampling schemes used for different experimental configurations.*

972

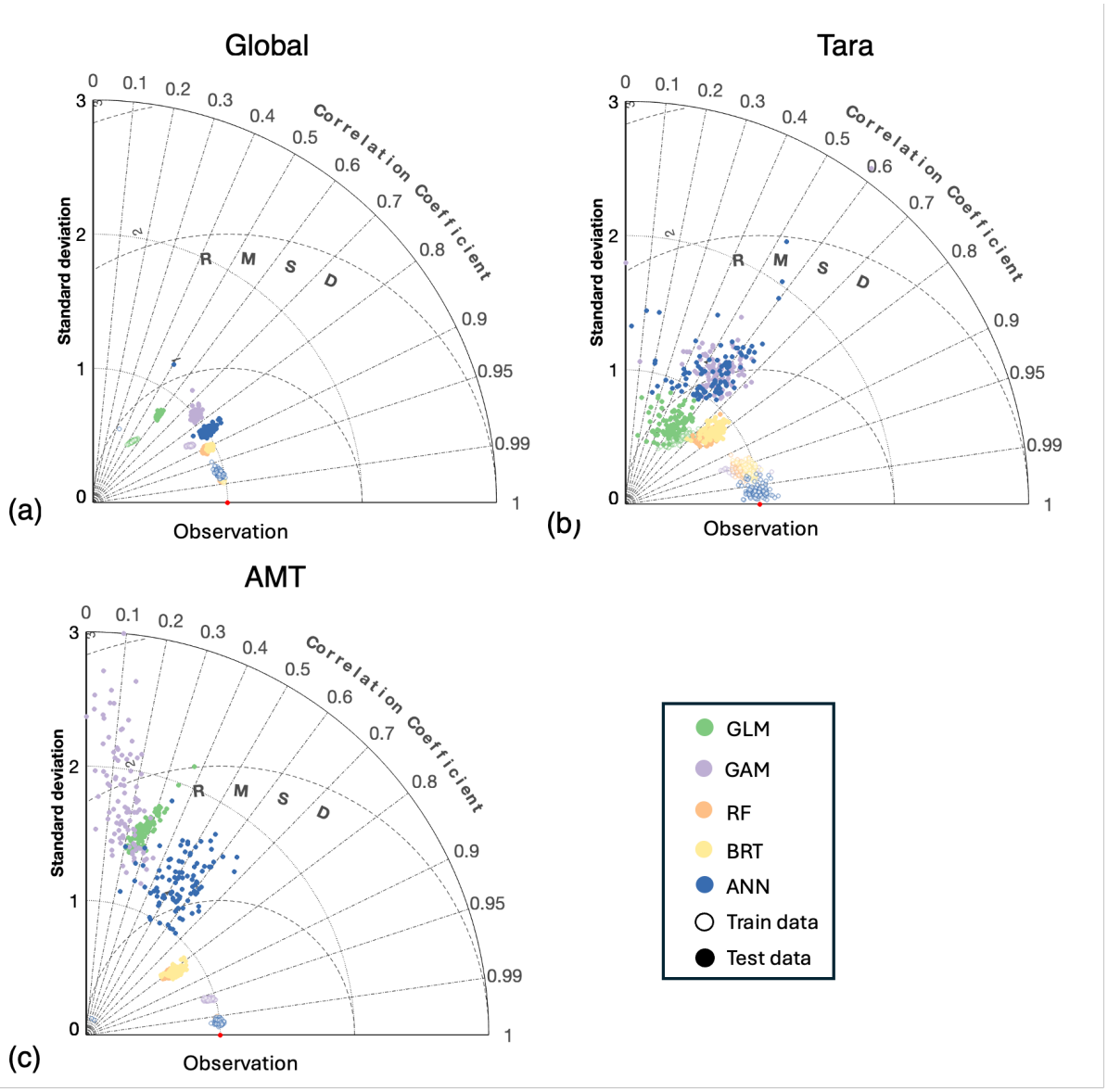

Figure S4: Model performances of SDMs for picoeukaryotes in 100 bootstrap runs based on global datasets (a), AMT datasets (b), and Tara Ocean datasets (c). Dots represent the predictions on training datasets and the crosses represent the testing datasets. In this case, the standard deviations have been normalized by dividing them by the standard deviations of the observations.

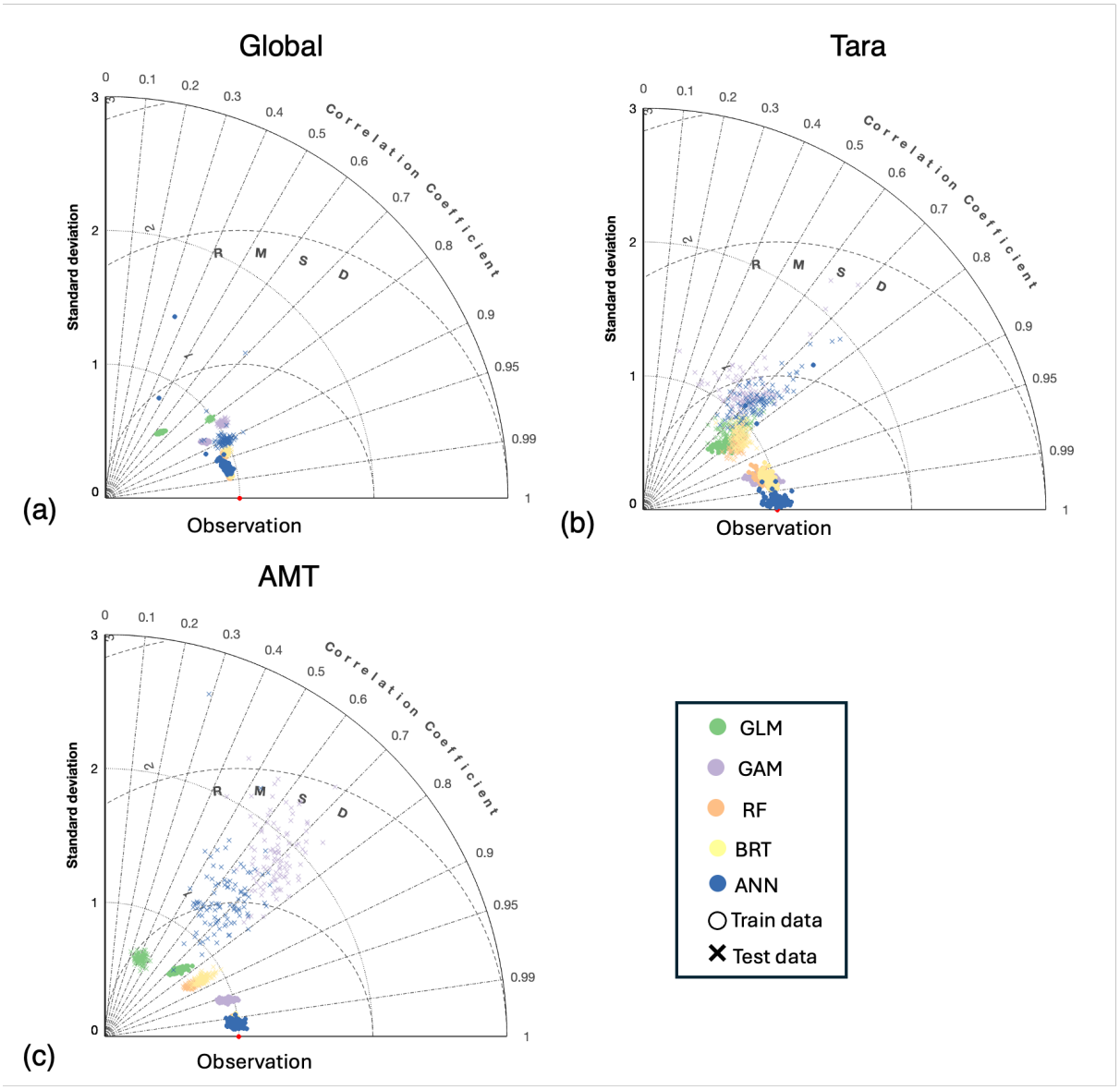

Figure S5: Model performances of SDMs for prokaryotes in 100 bootstrap runs based on global datasets (a), AMT datasets (b), and Tara Ocean datasets (c). Dots represent the predictions on training datasets and the crosses represent the testing datasets. In this case, the standard deviations have been normalized by dividing them by the standard deviations of the observations.

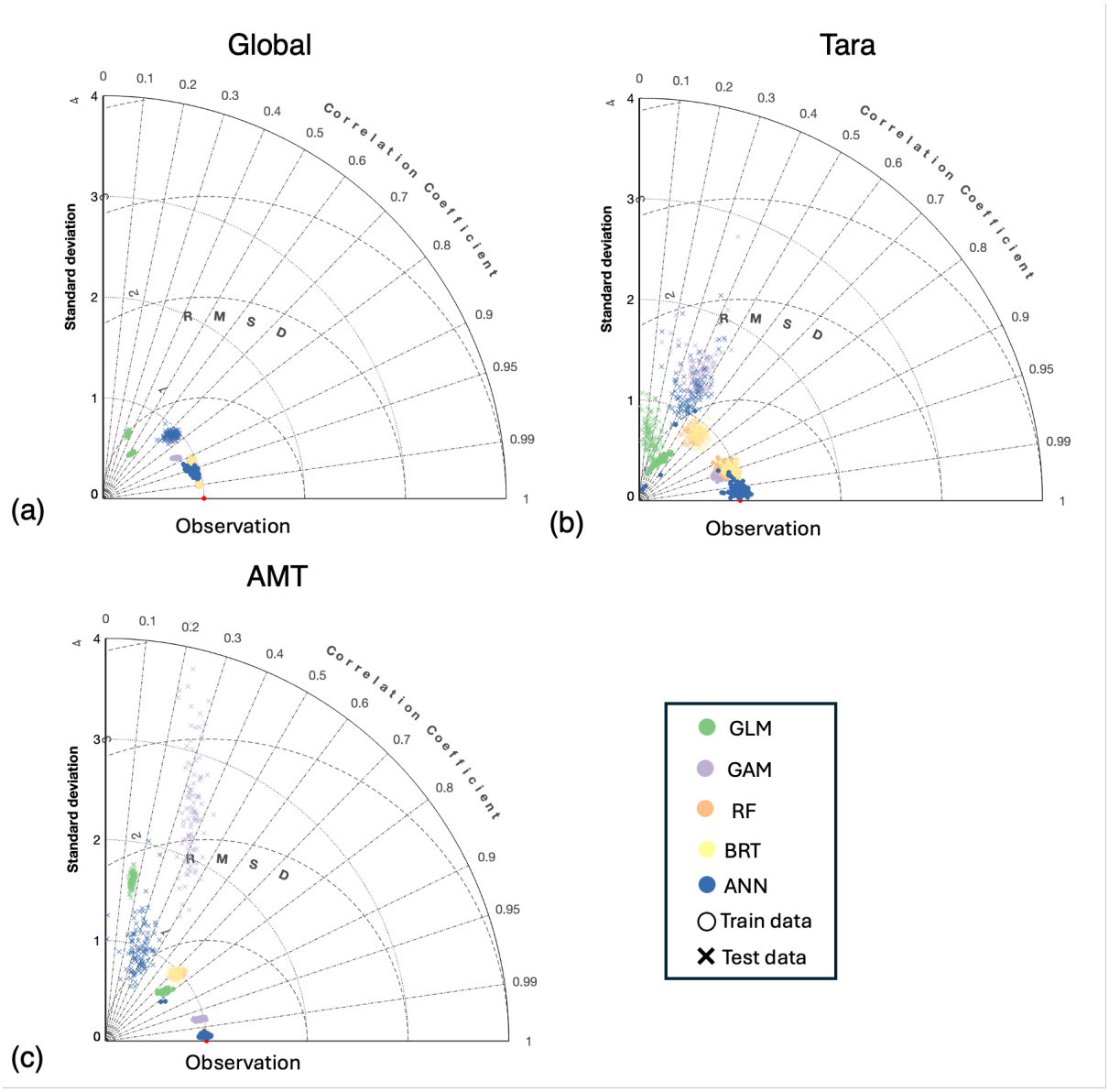

Figure S6: Model performances of SDMs for coccolithophores in 100 bootstrap runs based on global datasets (a), AMT datasets (b), and Tara Ocean datasets (c). Dots represent the predictions on training datasets and the crosses represent the testing datasets. In this case, the standard deviations have been normalized by dividing them by the standard deviations of the observations.

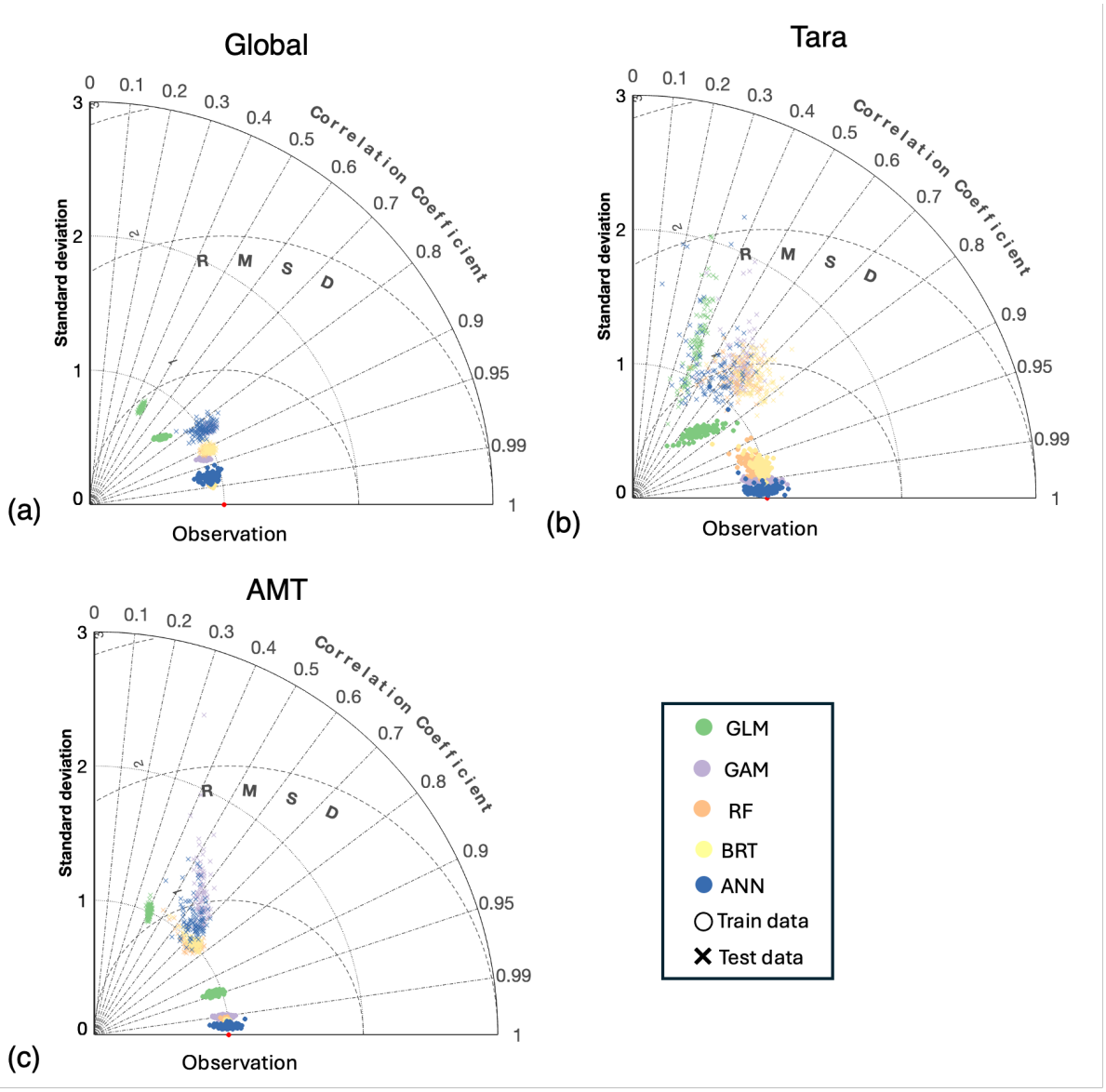

Figure S7: Model performances of SDMs for diatoms in 100 bootstrap runs based on global datasets (a), AMT datasets (b), and Tara Ocean datasets (c). Dots represent the predictions on training datasets and the crosses represent the testing datasets. In this case, the standard deviations have been normalized by dividing them by the standard deviations of the observations.

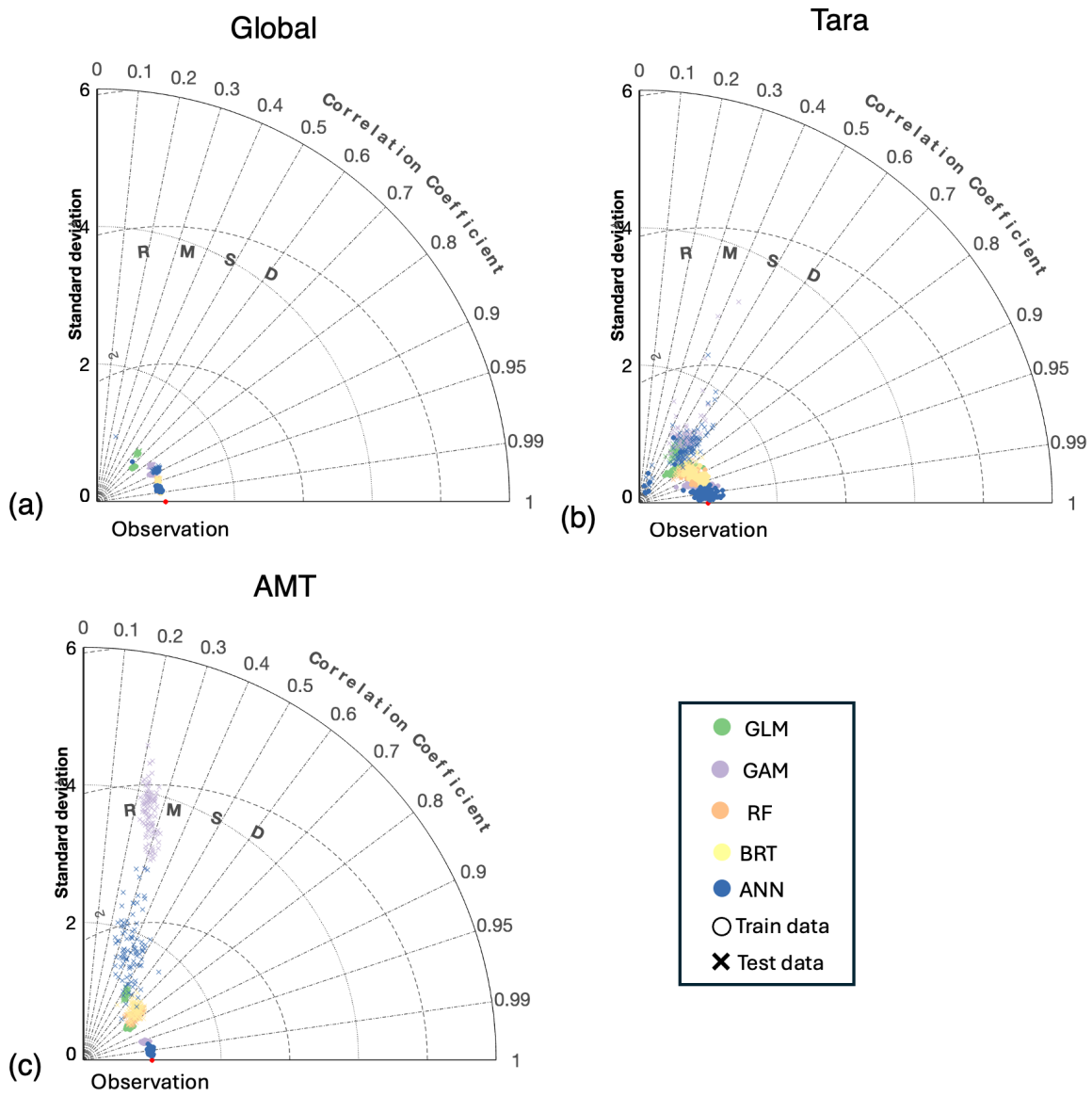

Figure S8: Model performances of SDMs for diazotrophs in 100 bootstrap runs based on global datasets (a), AMT datasets (b), and Tara Ocean datasets (c). Dots represent the predictions on training datasets and the crosses represent the testing datasets. In this case, the standard deviations have been normalized by dividing them by the standard deviations of the observations.

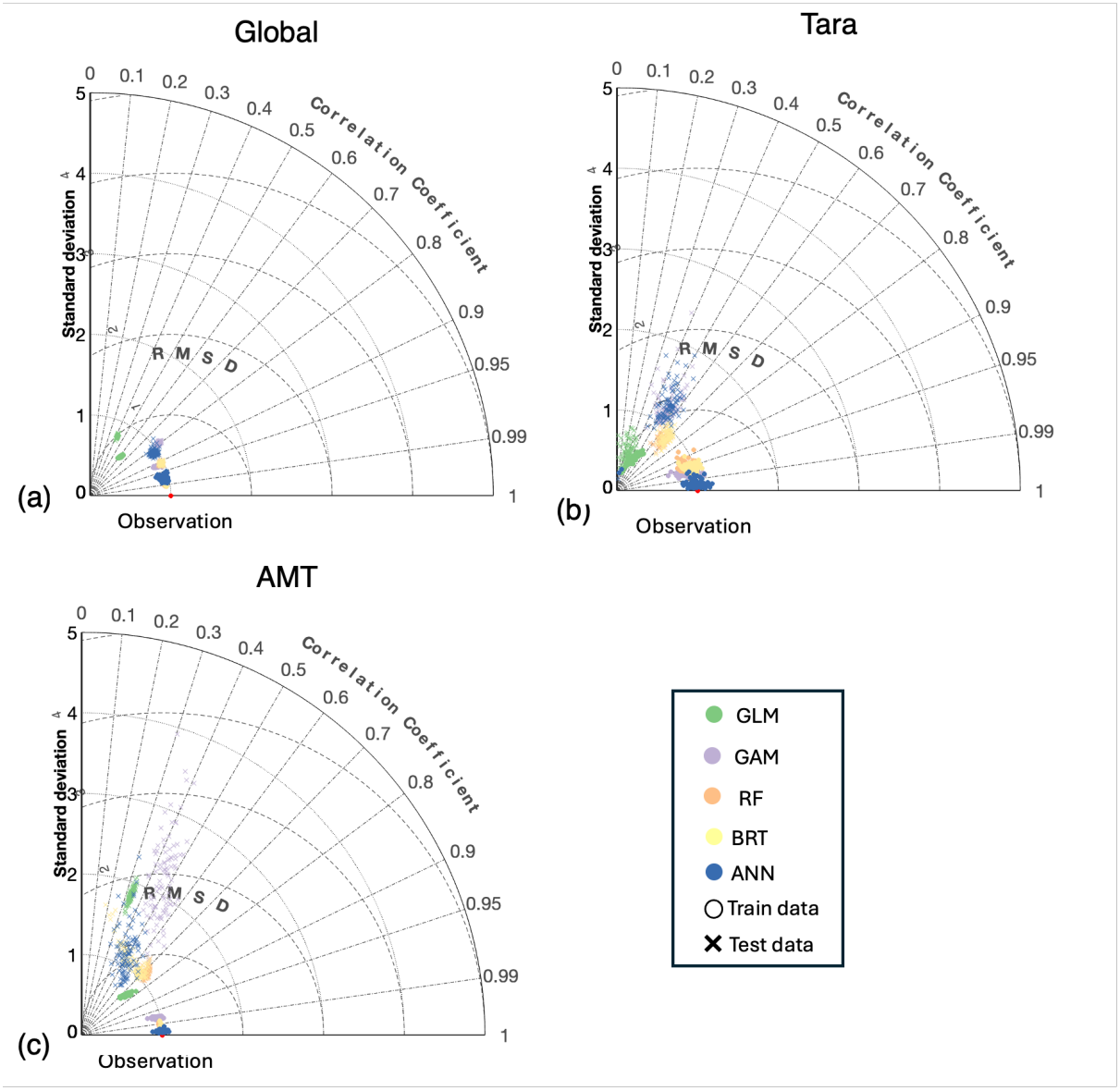

Figure S9: Model performances of SDMs for dinoflagellates in 100 bootstrap runs based on global datasets (a), AMT datasets (b), and Tara Ocean datasets (c). Dots represent the predictions on training datasets and the crosses represent the testing datasets. In this case, the standard deviations have been normalized by dividing them by the standard deviations of the observations.

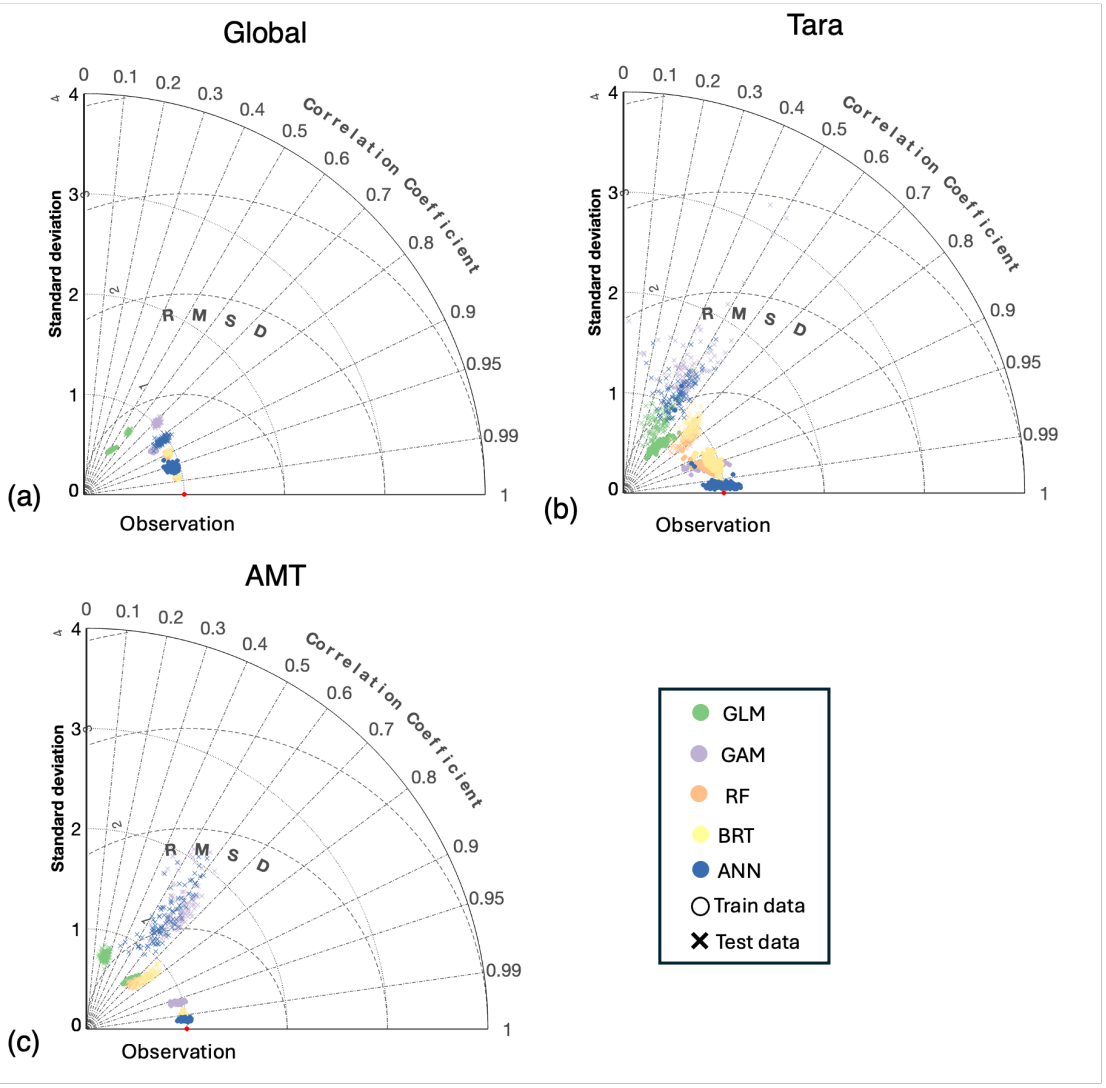

Figure S10: Model performances of SDMs for zooplankton in 100 bootstrap runs based on global datasets (a), AMT datasets (b), and Tara Ocean datasets (c). Dots represent the predictions on training datasets and the crosses represent the testing datasets. In this case, the standard deviations have been normalized by dividing them by the standard deviations of the observations.

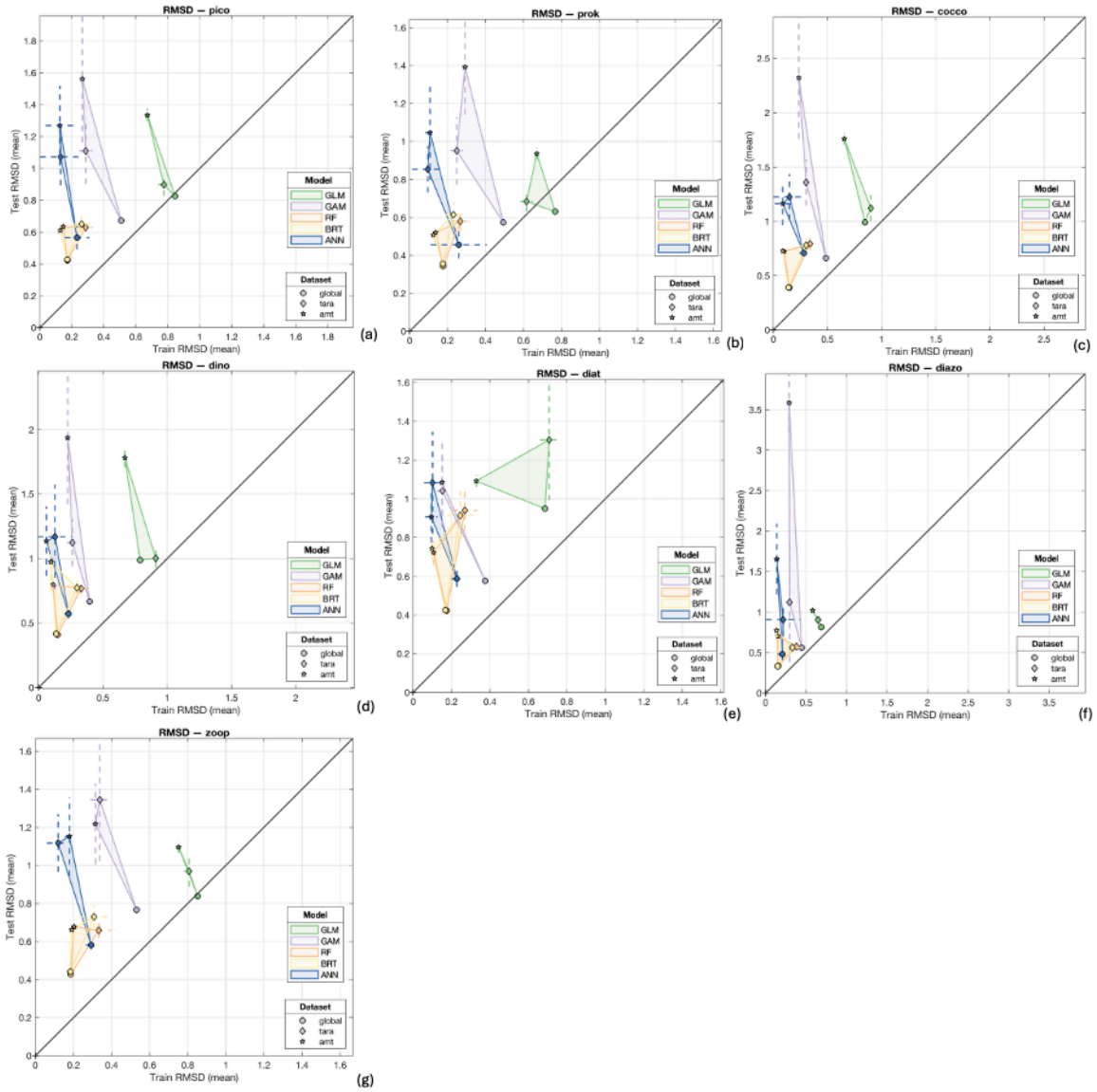

Figure S11. Train–test RMSD for seven plankton functional groups: (a) pico, (b) prok, (c) cocco, (d) dino, (e) diat, (f) diazo, and (g) zoop. Points show the mean RMSD from 100 bootstrap resamples; dashed crossbars indicate ±1 SD (horizontal = train, vertical = test). Marker color denotes model and marker shape denotes dataset (global, tara, amt). Thin lines connect the paired train–test means for each model–dataset, translucent patches outline the model-wise convex hull across datasets, and the 1:1 line indicates equal train–test performance.

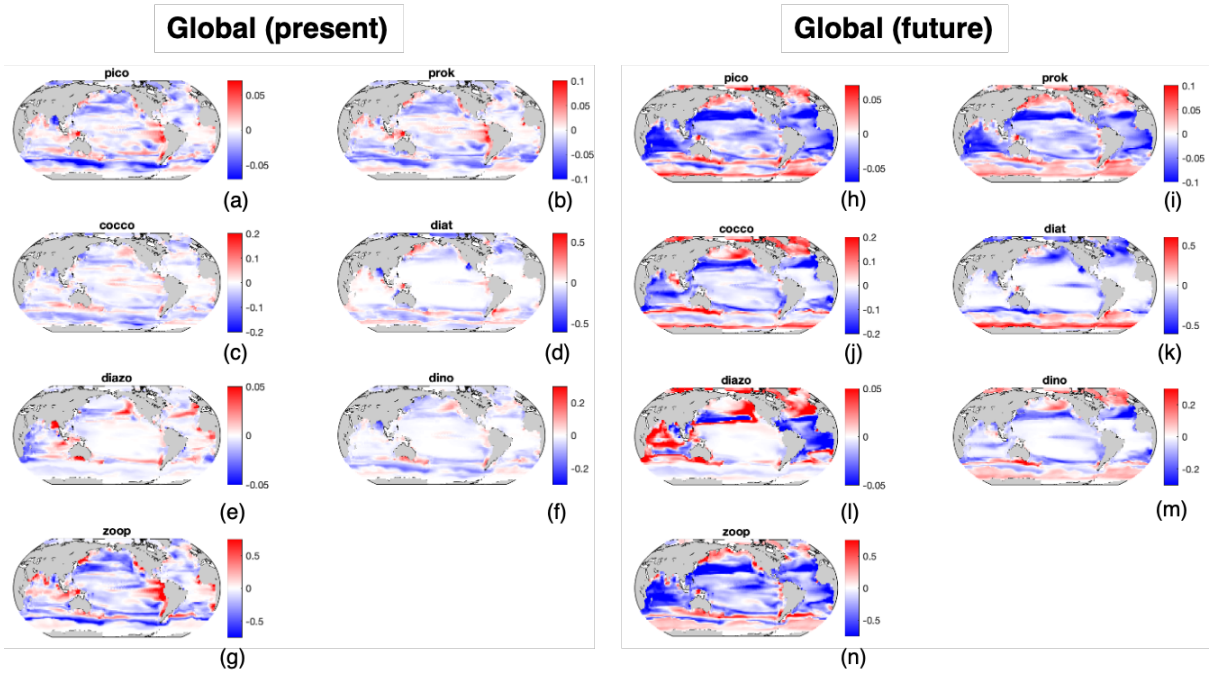

Figure S12. Residual map for RF models in the present (a-g) and future (h-n) ocean based on the Global dataset.

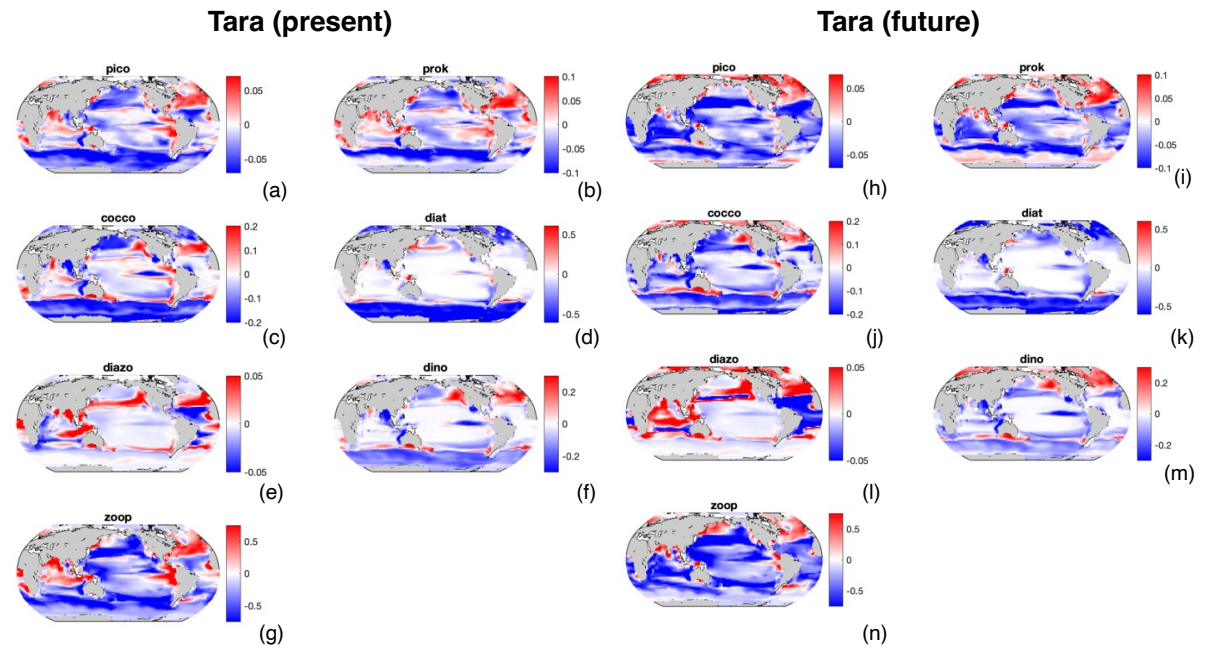

Figure S13. Residual map for RF models in the present (a-g) and future (h-n) ocean based on Tara datasets.

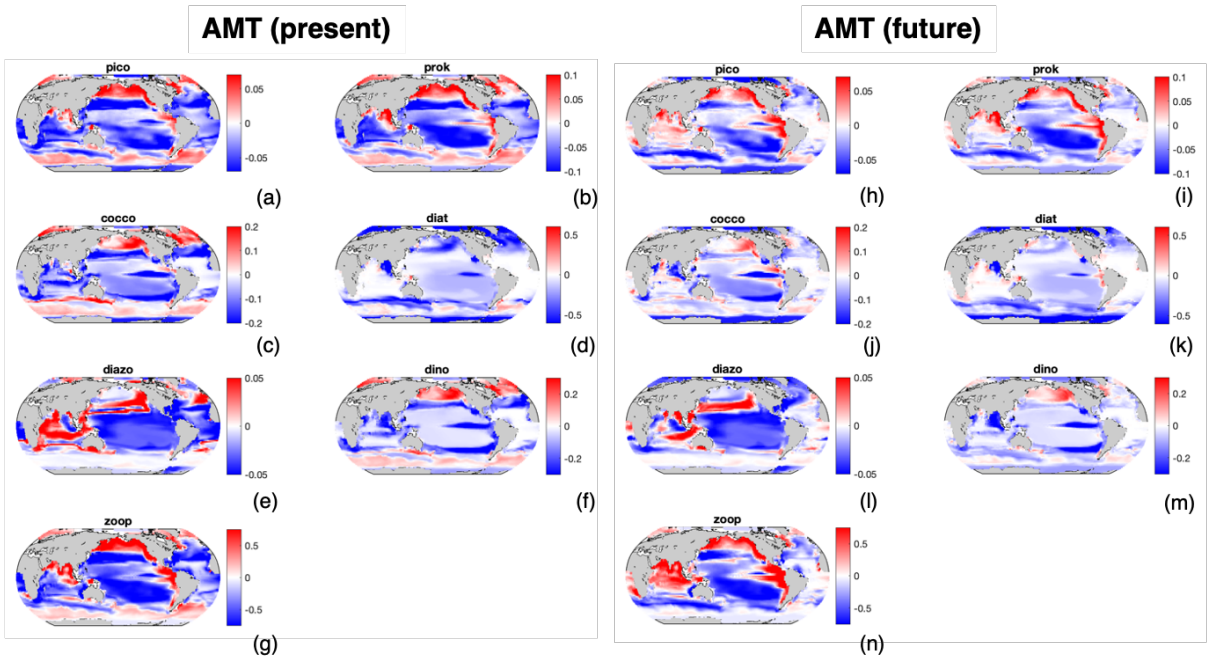

1025

1026

1027 *Figure S14. Residual map for RF models in the present (a-g) and future (h-n) ocean based on AMT datasets.*

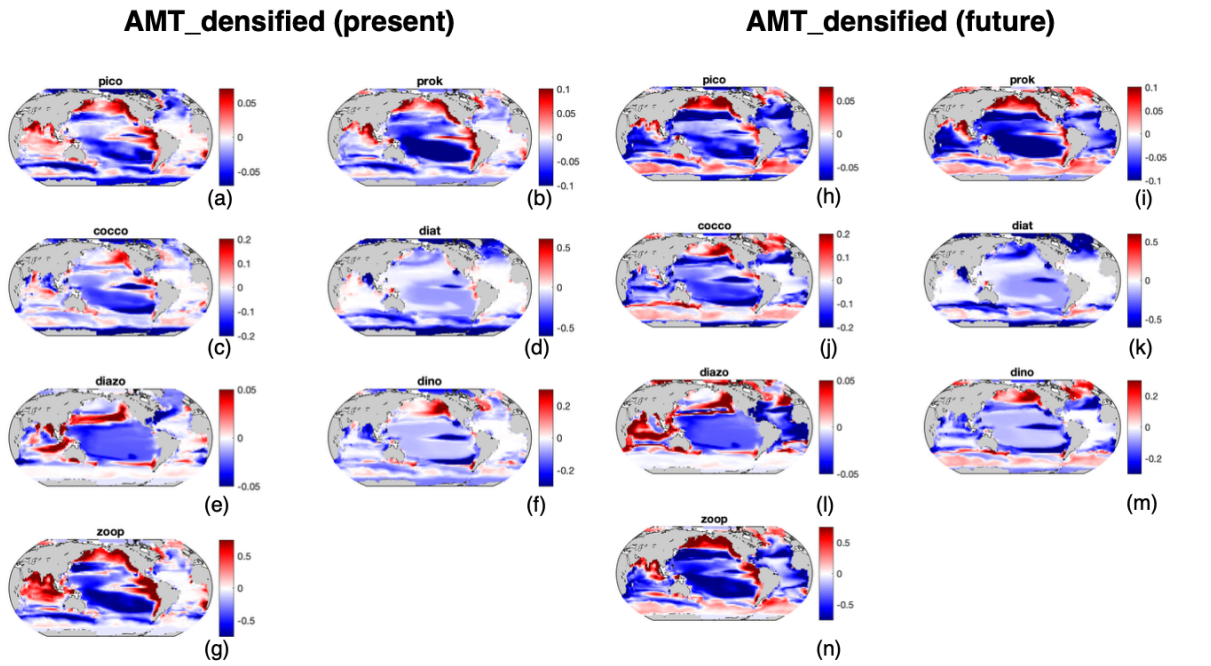

1028

1029 *Figure S15. Residual map for RF models in the present (a-g) and future (h-n) ocean based on AMT-densified*
1030 *datasets.*

1031

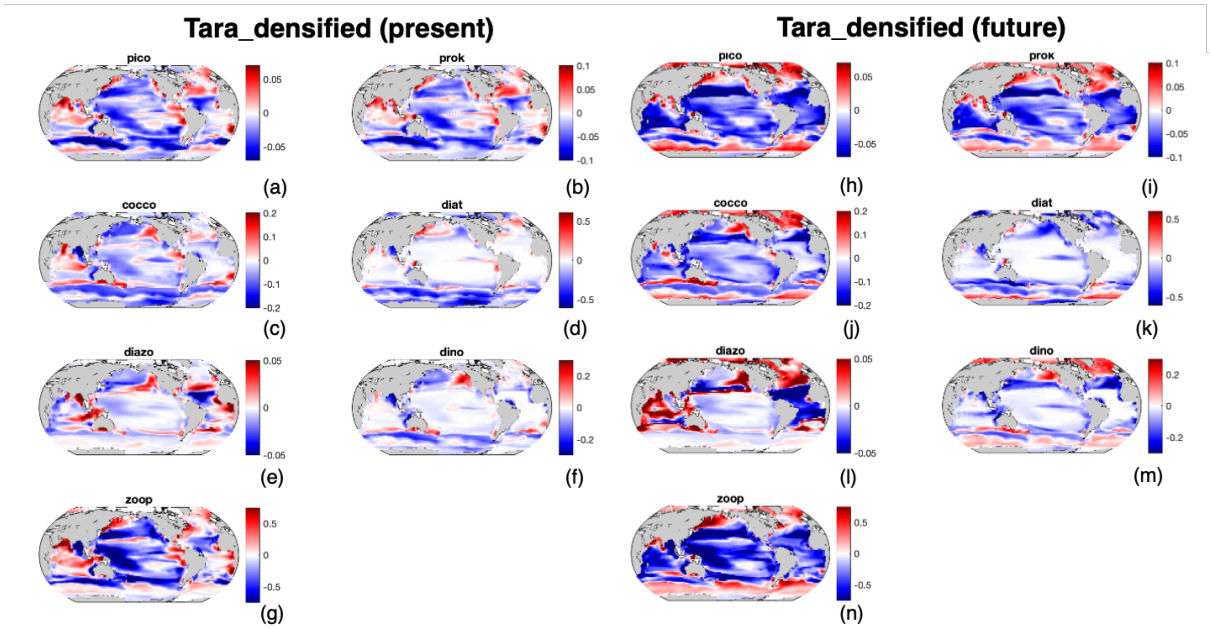

Figure S16. Residual map for RF models in the present (a-g) and future (h-n) ocean based on Tara-densified datasets.

Table S1 Summary of hyperparameter options in SDMs

RF		BRT		ANN	
parameter	options	parameter	options	parameter	options
n_estimator[a]	100, 200, 300	n_estimator	100, 200, 300	hidden_layer_sizes[f]	(100, 100), (100, 50), (50, 25)
max_depth[b]	None, 10, 20	max_depth	3, 4, 5	learning_rate[g]	0.01, 0.001, 0.0001
min_samples_split[c]	2, 5, 10	min_samples_split	2, 5, 10	num_epochs[h]	200, 500, 1000
max_feature[d]	1, 'sqrt', 'log2'	learning_rate[e]	0.05, 0.1, 0.2		

a: Specifies the number of trees in the forest, affecting model accuracy and stability

b: Limits the maximum depth of each tree to control complexity and prevent overfitting.

c: Sets the minimum number of samples required to split an internal node, helping to regulate model granularity

d: Number of features considered for each split, influencing diversity among trees.

e: Shrinkage factor applied to each tree's contribution to reduce overfitting.

f: Number and size of layers in the neural network, controlling model capacity and complexity.

g: Rate at which weights are updated during training, impacting convergence speed.

h: Number of times the training data is passed through the network, influencing training thoroughness.

Table S2 Summary of weights used in weighted SDM

Cluster	Region	Train datasets	Fraction of ocean area	Number of sampling points	Weights
1	North Pacific subtropic gyre and 40S	AMT	0.16	124	0.0013
2	Southern Ocean		0.12	9	0.0137
3	Indian ocean, tropical Pacific and South subtropical Atlantic		0.44	166	0.0027
4	Arctic Ocean		0.02	NA[a]	NA[a]
5	subpolar Pacific and Atlantic		0.12	96	0.0012
6	Tropical and North subtropical Atlantic		0.13	829	0.0002

1	North Pacific subtropic gyre and 40S		0.16	8	0.0200
2	Southern Ocean		0.12	4	0.0309
3	Indian ocean, tropical Pacific and South subtropical Atlantic	Tara	0.44	66	0.0067
4	Arctic Ocean		0.02	15	0.0016
5	subpolar Pacific and Atlantic		0.12	18	0.0065
6	Tropical and North subtropical Atlantic		0.13	20	0.0067
1	North Pacific subtropic gyre and 40S		0.16	369	0.0004
2	Southern Ocean		0.12	84	0.0015
3	Indian ocean, tropical Pacific and South subtropical Atlantic	Global dataset	0.44	1479	0.0003
4	Arctic Ocean		0.02	8	0.0030
5	subpolar Pacific and Atlantic		0.12	346	0.0003
6	Tropical and North subtropical Atlantic		0.13	881	0.0002

a: no data available

Pedregosa, F., Varoquaux, G., Gramfort, A., Michel, V., Thirion, B., Grisel, O., Blondel, M., Prettenhofer, P., Weiss, R., & Dubourg, V. (2011). Scikit-learn: Machine learning in Python. *the Journal of machine Learning research*, *12*, 2825-2830.